CO_2 refrigeration system heat recovery and thermal storage modelling for space heating provision in supermarkets: An integrated approach

Georgios Maouris[a], Emilio Jose Sarabia Escriva[b], Salvador Acha[a], Nilay Shah[a], Christos N. Markides[a]

[a] *Department of Chemical Engineering, Imperial College London, London SW7 2AZ, UK*

[b] *Termodinàmica Aplicada, Universitat Politècnica de València, 46022 València, Spain*

N.B.: This is the ACCEPTED MANUSCRIPT version of this article. The final, published version of the article can be found at: https://doi.org/10.1016/j.apenergy.2020.114722

Abstract

The large amount of recoverable heat from CO_2 refrigeration systems has led UK food retailers to examine the prospect of using refrigeration integrated heating and cooling systems to provide both the space heating and cooling to food cabinets in supermarkets. This study assesses the performance of a refrigeration integrated heating and cooling system installation with thermal storage in a UK supermarket. This is achieved by developing a thermal storage model and integrating it into a pre-existing CO_2 booster refrigeration model. Five scenarios involving different configurations and operation strategies are assessed to understand the techo-economic implications. The results indicate that the integrated heating and cooling system with thermal storage has the potential to reduce energy consumption by 17-18% and GHG emissions by 12-13% compared to conventional systems using a gas boiler for space heating. These reductions are achieved despite a marginal increase of 2-3% in annual operating costs. The maximum amount of heat that can be stored and utilised is constrained by the refrigeration system compressor capacity. These findings suggest that refrigeration integrated heating and cooling systems with thermal storage are a viable heating and cooling strategy that can significantly reduce the environmental footprint of supermarket space heating provision and under the adequate circumstances can forsake the use of conventional fossil-fuel (natural gas) boiler systems in food retail buildings.

Keywords: CO_2 refrigeration, supermarkets, heat recovery, thermal storage, natural refrigerants, integrated heating and cooling

Nomenclature

Abbreviations

CO_2	Carbon dioxide
CO_{2e}	Carbon dioxide equivalent
COP	Coefficient of performance
DNO	Distribution network operator
GHG	Greenhouse gas
GWP	Global warming potential
HFC	Hydrofluorocarbons
HP	High pressure
LP	Low pressure
LT	Low temperature
LTHW	Low temperature hot water
MT	Medium temperature
RIHC	Refrigeration integrated heating and cooling

Symbols

Δx	Thickness of each layer of the discretized buffer vessel (m)
ρ	Density (kg m^{-3})
A_d	Cross-sectional area of the buffer vessel (m^2)
A_{ls}	Lateral surface area of the buffer vessel (m^2)
c_p	Specific heat capacity at constant pressure (kJ kg^{-1} K^{-1})
h	Specific enthalpy (kJ kg^{-1})
k	Thermal conductivity coefficient (W m^{-1} K^{-1})
M	Total mass of water inside the buffer vessel (kg)
$\dot{m}$	Mass flow rate (kg s^{-1})
N	Number of layers used for the discretization of the buffer vessel
p	Pressure (bar)
$\dot{Q}$	Heat transfer rate (W)
T	Temperature (°C)
T_j^n	Temperature at time n of the layer j of the buffer vessel (°C)

t	Time
U	Overall heat transfer coefficient (W m^{-2} K^{-1})
V	Volume (m^3)
$\dot{W}$	Power (W)

Subscripts

BV	Buffer vessel
BVC	Discharging side of thermal storage system
BVH	Charging side of thermal storage system
destr	Destratification
DSH	Desuperheater
evap	Evaporator
ext	Exterior
GC	Gas cooler
HR	Heat recovery
IN	Inlet
opt	Optimal
OUT	Outlet
ret	Return flow
sat	Saturated
sup	Supply flow

1. Introduction

Over the last decades, there has been a growing level of concern regarding the depletion of fossil fuels and the associated emissions, leading many countries to set ambitious emission reduction targets (IPCC, 2014). In the UK, a target of at least 80% reduction of GHG emissions by 2050 compared to 1990 levels was established by the UK government with the legally binding Climate Change Act in 2008 (Fankhauser, Averchenkova & Finnegan, 2018).

The food retail industry is among the leading commercial energy consumers in the UK as it is responsible for approximately 3% of the overall electricity consumption and 1% of the total GHG emissions in the UK (The Carbon Trust, 2010). Supermarket refrigeration systems are considered as one of the industry's areas with the highest potential to contribute to the reduction of GHG emissions. They are associated with indirect GHG emissions as they account for approximately 50% of the total electricity consumed in a supermarket (Mylona et al., 2017). Additionally, as the supermarket refrigeration systems in the UK predominantly use HFC refrigerants, around 30% of their total emissions are associated with direct GHG emissions due to refrigerant leakages (Tassou et al., 2011). The significant amount of direct emissions combined with new legislation designed to phase-out HFC refrigerants have shifted the focus of the industry towards refrigeration systems using natural refrigerants such as CO_2 (Efstratiadi et al., 2019). In particular, the number of installations of CO_2 transcritical systems in supermarkets has been steadily increasing over the last years (Skacanova & Gkizelis, 2018) and is expected to continue to grow for the foreseeable future (Markets and Markets, 2019).

The re-emergence of CO_2 as a refrigerant over the last decades can be largely attributed to the fact that it is a natural substance. This is translated to a zero Ozone Depletion Potential and a global warming potential (GWP) of one. This is minimal compared to the best synthetic refrigerants such as R152a and R32 which have a GWP of 124 (Linde Gas, 2019b) and 675 (Linde Gas, 2019a) respectively. Compared to other natural refrigerants, CO_2 is unique because it is neither flammable nor toxic (Maina & Huan 2015). However, the main characteristic that separates CO_2 from the other refrigerants is the comparably low temperature (31.0 °C) and high pressure (73.8 bar) of its critical point (Markides, White & Handagama, 2017). This signifies that the heat rejection process of the refrigeration cycle needs to be performed in the transcritical region at ambient temperatures close or above the critical temperature (Sawalha, 2008). Another differentiating characteristic of CO_2 as a refrigerant is the relatively high pressure (5.2 bar) of its triple point which means that the CO_2 refrigeration cycle is required to operate at high pressures, larger than 5.2 bar, to avoid the solidification of the refrigerant (Danfoss, 2008).

The growing number of CO_2 booster refrigeration system installations has created an excellent opportunity for heat recovery due to their high operating pressures especially when they are operating in transcritical mode (Skacanova & Gkizelis, 2018). According to Ge & Tassou (2011), heat recovery from a CO_2 booster refrigeration system could cover 40% of the total space heating demand of a supermarket in the North England. The large amount of heat that can be recovered has led many researchers to examine the possibility that a CO_2 refrigeration system could provide

both the heating demand to the store and the cooling to the food cabinets. A major challenge in order to achieve that is the mismatch between the supermarket's peak heating and cooling demands (Wallace, 2013).

Sawalha (2013) developed a computer model to assess the performance of a CO_2 transcritical booster system which is exclusively responsible for the provision of space heating to an average-size supermarket in Sweden. The results obtained from the model suggested that the energy usage of the supermarket would be slightly reduced if a CO_2 booster system with heat recovery was used for the provision of space heating rather than a conventional system using R404A for refrigeration and a heat pump for heating.

A computer model was developed by Shi et al. (2017) using MATLAB to examine the performance of a similar system for an average supermarket in the Netherlands. The results obtained from this model indicated that a refrigeration system could satisfy the heating demand of a supermarket in the Netherlands without heat supplementation from other heating devices. The results also suggested that providing the cooling and the space heating exclusively by the refrigeration system would lead to 13% energy savings annually compared to a combination of a refrigeration system and a gas boiler.

Another model was developed by Polzot, D'Agaro & Cortella (2017) using the TRNSYS software (TRNSYS, 2019) to evaluate the performance of a CO_2 booster refrigeration system which would be responsible for the provision of both the space heating and the hot water (DHW) to the supermarket. The energy consumption of the system was compared against a baseline system consisting of a cascade R134a/ CO_2 system for refrigeration and a R410A heat pump for space heating and DHW. The results obtained from this model suggested that the use of the CO_2 booster transcritical system for cooling, heating and DHW would result in a 3.6-6.5% reduction of annual energy consumption compared to the baseline system for the locations with high temperature fluctuations. However, it would be less efficient than the baseline system for the location with low temperature variations.

The performance of an integrated CO_2 booster system for refrigeration, heating and air-conditioning (all-in-one system) was examined by Karampour & Sawalha (2016a) using data obtained from an all-in-one system installation in a Swedish supermarket. The results obtained suggested that the recoverable heat from the system was sufficient to provide hot water at a temperature of 55-60 °C during the whole year and space heating for ambient temperatures as low as -15 °C. For lower temperatures, the additional space heating demand would be fulfilled by district heating. Additionally, the authors found that the air-conditioning system operated with high COP values for ambient temperature larger than 25 °C and the COP for heating was within similar range with most of the commercial heat pumps (Karampour & Sawalha, 2016b). Thus, Karampour & Sawalha (2016b) advocated that the all-in-one solution would provide substantial environmental benefits for supermarkets located in cold or mild climates.

The control strategies for heat recovery from CO_2 booster refrigeration systems discussed in the previous paragraphs were focused on satisfying the instantaneous heating demand of the supermarkets. However, they could not take advantage of the excess amount of recoverable heat produced during low heating demand periods. This can be achieved by integrating a thermal storage system to the refrigeration system which would enable the storage of the

excess recoverable heat for subsequent use (Rahman, Fumo & Smith, 2015). Different approaches for the development of thermal storage system models were suggested by Raccanello, Rech & Lazzaretto (2019) including zero, quasi-one and one-dimensional models. A one-dimensional model was developed and experimentally validated by Angrisani et al. (2014) using TRNSYS (TRNSYS, 2019) in order to calculate the temperature stratification inside a thermal storage tank equipped with multiple heat exchangers. A simplified mathematical model in order to determine the size of the storage tank for combined cooling, heating and power (CCHP) systems using MATLAB was proposed by Rahman, Fumo & Smith (2015). Another MATLAB model to calculate the temperature stratification of a storage tank working in conjunction with an absorption chiller and a solar collector was developed by Buckley (2012).

Nöding et al. (2016) developed a model incorporating thermal storage into a CO_2 booster refrigeration system which exclusively covers the heating demand of a supermarket. The model, which was developed in the object-oriented Modelica language, enabled the timewise separation of heat production and heat demand. According to Nöding et al. (2016), the integration of thermal storage would result in power consumption savings of 8.5% for an average January day in Braunschweig (Germany) compared to the baseline strategy for which the heat recovered from the refrigeration system should match the heating demand instantaneously.

The performance of an all-in-one CO_2 booster refrigeration with parallel compression, integrated with two thermal storage tanks for heating and hot water was modelled and calibrated by D'Agaro, Coppola & Cortella (2019) based on field measurements obtained from a small size supermarket located at northern Italy. Depending on operating conditions, the electricity consumption of the refrigeration system was predicted within a -4% and -9% error. Based on this model, D'Agaro, Coppola & Cortella (2019) simulated four different control strategies for heat recovery which indicated that measures taken to increase the recoverable heat from the refrigeration systems could lead to energy savings between 5.9% and 7.3%. However, limited work has been carried out to evaluate the performance of similar systems in supermarkets located at regions with colder climates such as the UK.

A Refrigeration Integrated Heating and Cooling (RIHC) system can be defined as a CO_2 booster refrigeration system which is responsible for the supply of both the space heating to the store and the cooling to the chilled and frozen food cabinets. As the UK is expected to rely even more heavily on renewable energy sources for electricity generation in the near future, the potential electrification of the heating provision to the supermarkets by using RIHC systems could significantly contribute to the optimisation of the future energy resources. Moreover, RIHC systems could potentially eliminate the need for gas boilers in supermarkets and consequently the reliance on natural gas; a dwindling fossil fuel resource. Thus, the aim of this paper is to study the performance of a RIHC system with thermal storage and evaluate its potential to reduce operating costs and carbon emissions for a UK supermarket compared to a conventional solution for which a gas boiler is used in order to provide the space heating.

The remainder of the paper is divided into three main sections. Section 2 includes a detailed description of the methodology used to develop a model in order to simulate the performance of a RIHC system with thermal storage. It also includes detailed descriptions of the five different control strategies investigated for heating and cooling the supermarket. Section 3 presents a comparison of the performance of the five strategies and an analysis of their behaviour during typical winter and summer days. Lastly, the key conclusions are summarised in Section 4 before areas for further work are highlighted.

2. Methodology

A thermal storage model was developed in order to calculate the temperature stratification inside a buffer vessel. The model uses the heat recovered from a supermarket refrigeration system and the heating demand of the same supermarket as inputs. The model developed was then integrated into the CO_2 booster refrigeration system developed by Sarabia Escriva et al. (2019) in order to simulate different control strategies for the provision of space heating and cooling to the food cabinets of a supermarket.

2.1. CO_2 booster refrigeration system

2.1.1. System description

Many researchers including Colombo et al. (2011) and Karampour & Sawalha (2014) have described the operation of a typical supermarket CO_2 booster refrigeration system (Figure 1). The system is responsible to maintain the frozen (LT) and chilled (MT) food cabinets at a specific temperature by absorbing heat through the LT and MT evaporators respectively. These evaporators are used in conjunction with expansion valves which ensure that the refrigerant exiting the evaporators is superheated. An LP compressor is used to raise the pressure of the refrigerant at the exit of the LT evaporator to the MT pressure before it is mixed with the refrigerant from the MT evaporator and the gas valve. The resulting gas mixture is then compressed by the HP compressors to the condenser (discharge) pressure. The heat rejection process from the refrigerant to the atmosphere is carried out by the condenser/gas cooler. An expansion valve located after the condenser/gas cooler is used to control its pressure. Lastly, the CO_2 refrigerant is throttled to a liquid-gas mixture before it enters the flash tank (receiver) where the mixture is separated to gas and liquid. The saturated liquid refrigerant at flash tank pressure is then distributed to the MT and LT evaporators where it is expanded to the corresponding pressure by different valves.

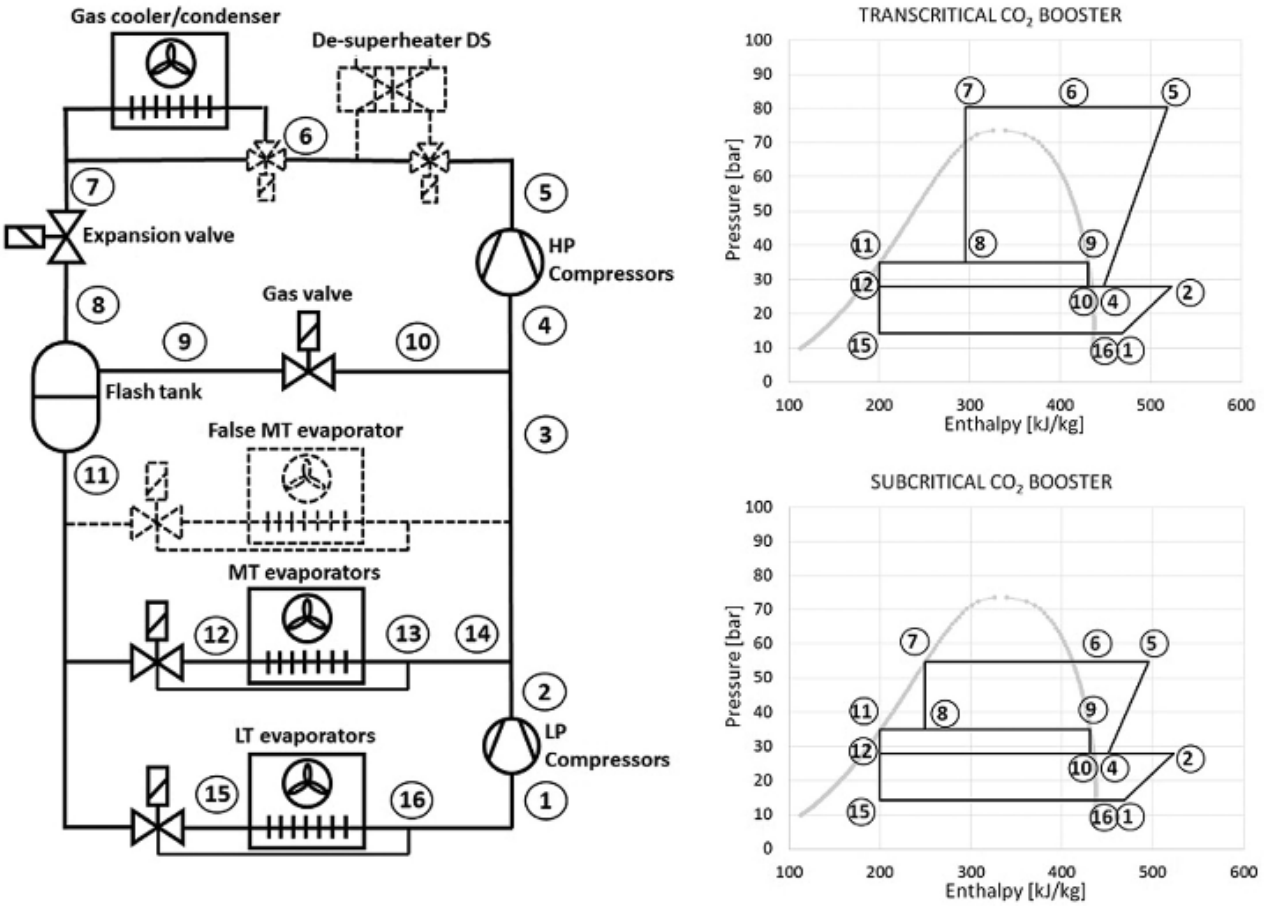

Figure 1. (Left) Schematic of a CO_2 booster refrigeration system. (Right) Pressure-enthalpy diagrams for transcritical and subcritical operation (Sarabia Escriva et al., 2019).

According to Gullo, Hafner & Cortella (2017), the optimal condenser pressure for the subcritical operation of the system can be specified as:

$$p_{GC,opt} = p_{sat}(T_{GC,exit}) \quad (1)$$

According to Sawalha (2013), the optimal discharge pressure when the system operates in the transcritical cycle can be calculated as:

$$p_{GC,opt} = 2.7 \cdot T_{GC,exit} - 6 \quad (2)$$

Before being rejected by the condenser/gas cooler, a portion of the heat can be recovered by the desuperheater. When the refrigeration system operates without control to increase the amount of recoverable heat, it is considered to be operating at floating condensing conditions (Sawalha, 2013). The topic of heat recovery will be further discussed in Section 2.1.3.

2.1.2. Model description

Sarabia Escriva et al. (2019) developed a steady-state model in order to simulate the behaviour of an existent CO_2 booster refrigeration system. The model was developed using telemetry data from a store located at the West Midlands region of the UK. According to Sarabia Escriva et al. (2019), a typical supermarket refrigeration system installation consists of two identical CO_2 booster refrigeration packs, responsible for the cooling of approximately the same number of chilled and frozen food cabinets. Thus, it was assumed by Sarabia Escriva et al. (2019) that the two packs have an equal electricity consumption at any given moment. The operating conditions of the different components of the refrigeration system were modelled by Sarabia Escriva et al. (2019) using telemetry data from the store under consideration between 2017 and 2018. The model was validated using real electricity consumption data from the same store. Despite a 11% average percentage error in instantaneous power input, the model managed to predict the annual energy consumption accurately with an error of only 0.12% for the supermarket installation under consideration.

2.1.3. Heat recovery

An effective control strategy to increase the amount of recoverable heat is essential for a supermarket CO_2 refrigeration integrated heating and cooling system. In the following paragraphs, the proposed control strategy by Danfoss (2010) will be explained. A similar strategy was also adopted by Sawalha (2013) and Shi et al. (2017).

Having in mind that the priority of the refrigeration system remains to provide sufficient cooling to the LT and MT cabinets, the recoverable heat from the refrigeration system can be increased by applying the following measures in order of priority:

a) Increase of condenser pressure:

As shown in Figure 2, a larger percentage of the heat rejected from the refrigeration system can be reclaimed by the desuperheater as the condenser pressure increases. This phenomenon is magnified when the system operates in transcritical mode, i.e., above the critical point (73.9 bar). It is important to note that despite the 120-bar design pressure of commercial CO_2 refrigeration plants, a pressure of 100 bar is commonly adopted in practice based on consultation with industry due to a combination of regulations and the inaccuracy of the pressure limiting switches. Thus, the adoption of a maximum condenser pressure for heat recovery larger than 100 bar would require paying a premium price for the refrigeration equipment with a higher maximum pressure. It would also pose challenges regarding the replacement of faulty equipment parts within a short timeframe.

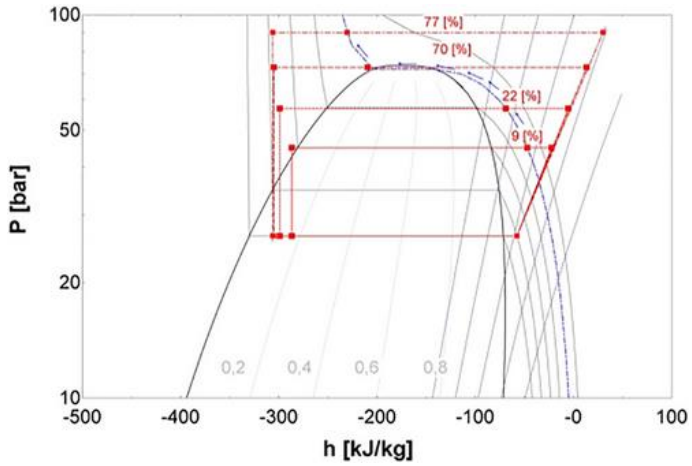

Figure 2. P-h diagram showing the percentage of recoverable heat from with different condenser pressures (Danfoss, 2010).

b) Reduction of gas cooler fan speed:

If the condenser pressure limit is reached and additional heat is required, the gas cooler fans are gradually slowed down leading to a higher refrigerant temperature and enthalpy at the exit of the condenser/gas cooler. Thus, a larger percentage of the heat can be recovered by the desuperheater before it is rejected from the system (Figure 3). The maximum amount of heat can be reclaimed when the gas cooler is completely bypassed and all the heat is rejected/reclaimed by the desuperheater.

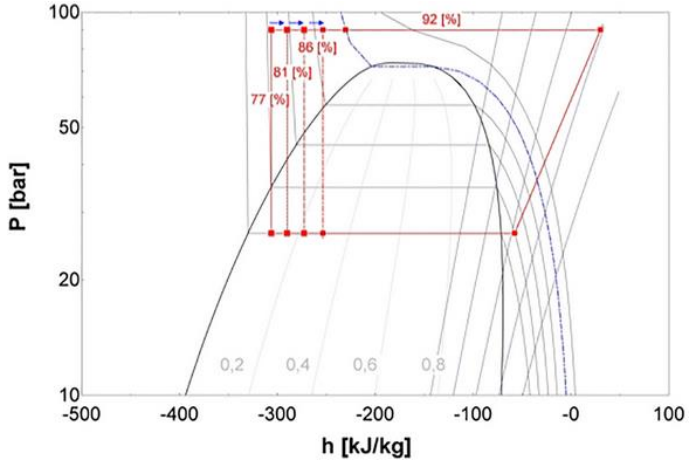

Figure 3. P-h diagram showing the fraction of recoverable heat as the gas cooler fan speed is reduced (Danfoss, 2010).

c) Use of a false load evaporator

If the recoverable heat from the refrigeration system is still insufficient when the gas cooler is bypassed, a false load MT evaporator can be used to further increase the amount of recoverable heat (Figure 1). This is achieved by displacing heat from the ambient air leading to a higher cooling load to the refrigeration system. In order to satisfy the additional cooling load, the mass flowrate at the HP compressors is increased accordingly and thus, an

increased amount of heat is rejected/reclaimed. However, the additional refrigeration requirements due to the false load evaporator lead to a reduction of the overall system efficiency.

2.2. Thermal storage system description

The performance of a RIHC system could be potentially improved by integrating a thermal storage system which would allow the exploitation of the heat recovered during periods when the recoverable heat exceeds the heating demand. A schematic of a thermal storage is shown in Figure 4 and can be divided into three parts:

a) Charging (primary) side:

As described in Section 2.1.1, heat can be recovered from the refrigeration system by integrating a desuperheater between the HP compressor and the condenser/gas cooler. The heat recovered is then transferred into the buffer vessel via the charging side of the thermal storage system. A temperature difference of at least 15 K between the supply and return flows of the charging side is maintained by using a variable speed water pump. This is achieved by adjusting the mass flowrate of the water depending on the amount of heat recovered by the refrigeration system. The variable speed water pump of the charging side is never turned off during the operation of the system. It rather operates at its minimum setting which is 10% of the maximum mass flowrate required during operation based on consultation with industry.

b) Buffer vessel:

The role of the buffer vessel is to act both as an intermediary between the charging and discharging sides and as a heat storage device when there is an excess amount of recoverable heat. The top of the buffer vessel is always maintained at a temperature of at least 45 °C, i.e., the minimum design LTHW supply temperature. Conversely, if the temperature of the buffer vessel exceeds 70 °C, the desuperheater three-way valve closes so that no heat recovered from the refrigeration system is transferred into the buffer vessel.

c) Discharging (secondary) side:

The discharging side of the thermal storage is responsible for the circulation of the LTHW so that adequate heating is provided to the store. This is ensured by using a variable water pump which enables the adjustment of the mass flowrate depending on the temperature at the top of the buffer vessel, i.e., the LTHW supply temperature.

Consistent with the work carried out by Sarabia Escriva et al. (2019), it was assumed that the heating demand was exclusively for space heating purposes neglecting the hot water requirements of the store. It should also be noted that as there are two identical CO_2 booster refrigeration packs providing the cooling to the frozen and chilled food cabinets, there are also two identical charging side circuits providing the heating to the buffer vessel at the same time.

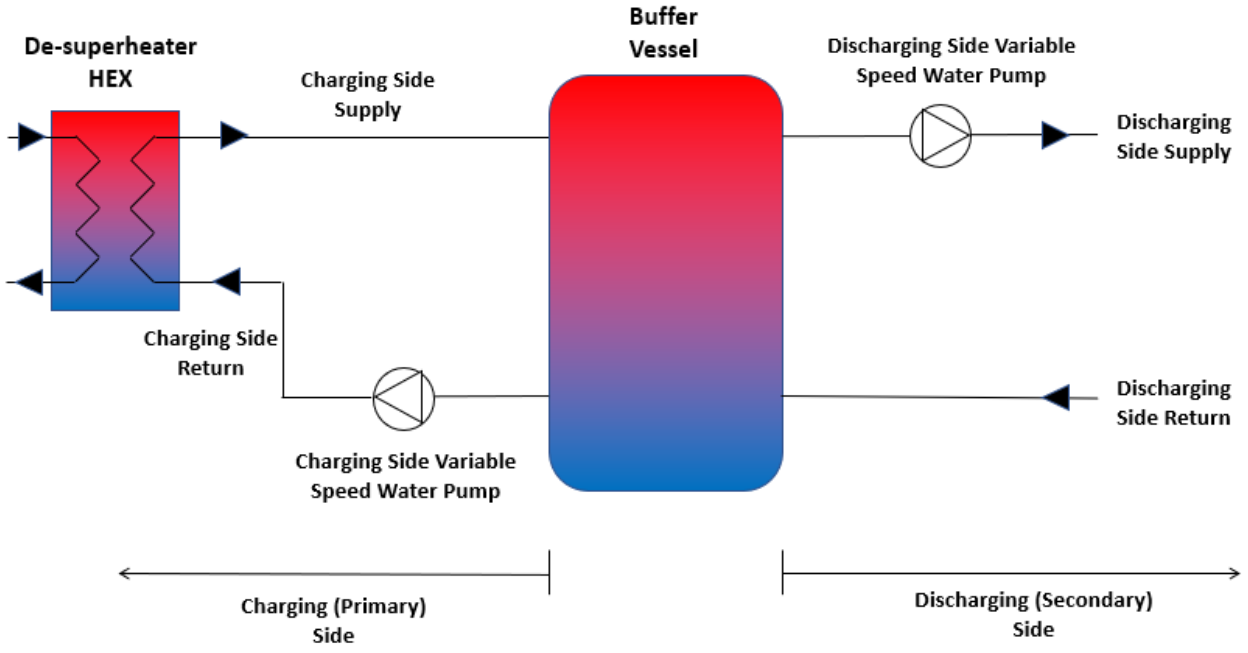

Figure 4. Schematic of the thermal storage system and its relationship with its primary and secondary side.

2.3. Thermal storage model

A one-dimensional model employing an implicit finite difference method was developed in order to simulate the thermal storage system described in the previous section. The model was developed in Scilab and was integrated into the CO_2 booster refrigeration system model developed by Sarabia Escriva et al. (2019).

2.3.1. One-dimensional model

A one-dimensional model was developed rather than a zero-dimensional or a quasi-one dimensional model as it incorporates the effects of heat conduction and mass transfer of the water inside the buffer vessel (Raccanello, Rech & Lazzaretto, 2019). The development of a one-dimensional model involves the discretization of the buffer vessel into N number of layers with an equal thickness Δx (Raccanello, Rech & Lazzaretto, 2019). As each layer has a uniform temperature, there is a temperature stratification inside the buffer vessel. A schematic representation of the discretized buffer vessel is shown in Figure 5.

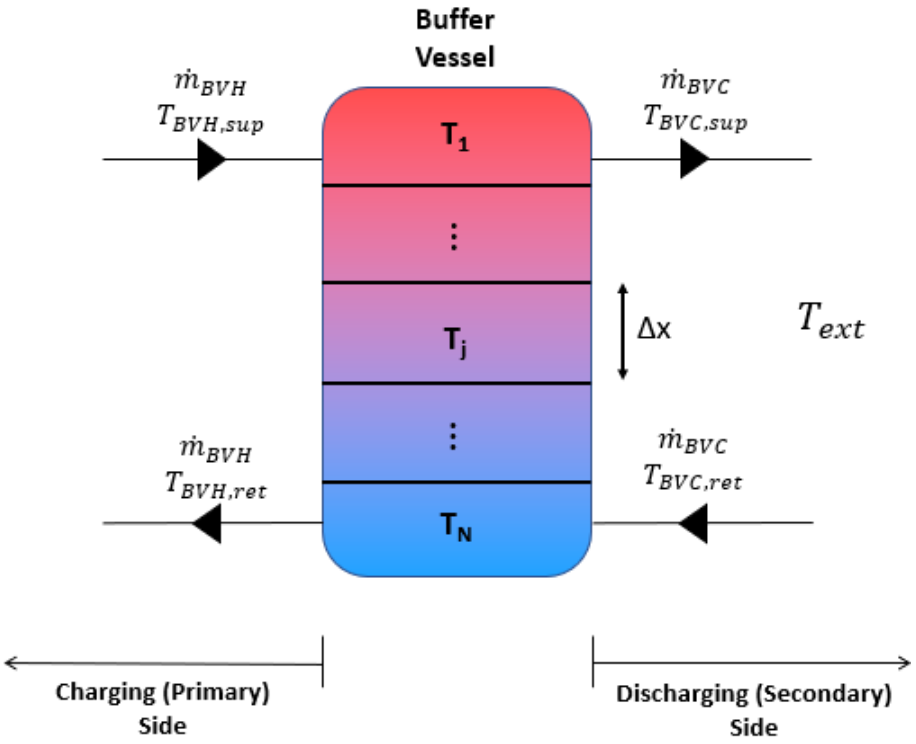

Figure 5. Schematic characterising the discretization of the buffer vessel for a one-dimensional model.

According to Raccanello, Rech & Lazzaretto (2019), the following energy balance equation must be satisfied for each layer:

$$M_j \cdot c_p \cdot \frac{dT_i}{dt} = \dot{m}_{BVH} \cdot c_p \cdot (T_{j-1} - T_j) + \dot{m}_{BVC} \cdot c_p \cdot (T_{j+1} - T_j) + k \cdot A_d \cdot \frac{1}{\Delta x} \cdot (T_{j-1} - T_j)$$

$$+k \cdot A_d \cdot \frac{1}{\Delta x} \cdot (T_{j+1} - T_j) - U \cdot \frac{A_{ls}}{N} \cdot (T_j - T_{ext}) \quad (3)$$

where:

$$M_j = \frac{M}{N} = \rho \cdot A_d \cdot \Delta x \quad (4)$$

Thus, a system of N energy balance equations with N number of unknowns is created which must be solved in order to obtain the temperature of each layer at a given time. The heat losses from the storage tank are accounted for by using an overall heat transfer coefficient for the buffer vessel (U).

A destratification conductivity (k_{destr}) equal to 0.285 W m^{-1} K^{-1} was also introduced into the model in order to improve its accuracy. The value adopted was based on the work carried out by Angrisani et al. (2014) who developed and calibrated a one-dimensional thermal storage model using experimental data. Thus, the overall thermal conductivity between the different layers was considered as:

$$k = k_{water} + k_{destr} \quad (5)$$

2.3.2. Implicit finite difference method

The energy balance equations obtained for each layer as described in the previous section can be characterized as ordinary differential equations. There are two main finite difference methods which can be utilized in order to solve this system of energy balance equations: a) the explicit method and b) the implicit method (Bui, 2010). Although the equations derived by using an explicit method are less computationally expensive to solve than those derived by using an implicit method, the explicit method is conditionally stable, i.e., the selection of the size of the timestep is constrained by the stability criterion (Davis, 2011). Conversely, the implicit method is unconditionally stable (Davis, 2011) and thus, less timesteps would be required to obtain the solution for a given time period compared to the explicit method.

As the thermal storage model would be used for the simulation of the temperature stratification inside the buffer vessel for a one-year period, the implicit method was determined as the most suitable method as it would significantly reduce the time required for the simulations compared to the explicit method. The choice of the implicit method is also consistent with the thermal storage models developed by Rahman, Fumo & Smith (2015) and Buckley (2012).

2.3.3. Formulation of the model equations

The key equations developed for the thermal storage model were the following:

a) Heat transfer from the desuperheater to the buffer vessel:

The heat input to the primary (hot) side of the desuperheater is calculated for each timestep by the CO_2 booster refrigeration model. According to Alfa Laval (2014), the heat losses from the heat exchanger to the atmosphere are minimal and therefore, can be neglected. Thus, the heat recovered from the refrigeration system is equal to the heat supplied to the buffer vessel:

$$\dot{Q}_{PHEX,OUT} = \dot{Q}_{PHEX,IN} \quad (6)$$

However, when the temperature of the top layer of the buffer vessel exceeds the upper allowable limit of 70 °C, the desuperheater three-way valve closes and no heat is transferred to the vessel.

b) Mass flowrate of charging side:

As mentioned in Section 2.2, the system aims to maintain a temperature difference of 15 K between the supply and the return flow of the charging side. Additionally, the temperature of the return flow of the charging side was assumed to be equal to the temperature of the bottom layer of the buffer vessel. Therefore, the temperature of the supply flow of the charging side, assumed to be entering the vessel at the top layer, was calculated as:

$$T_{BVH,sup} = T_{BVH,ret} + 15 \quad (7)$$

Thus, the mass flowrate was calculated as:

$$\dot{m}_{BVH} = \frac{\dot{Q}_{PHEX,OUT}}{c_p \cdot (T_{BVH,sup} - T_{BVH,ret})} \quad (8)$$

If the mass flowrate of the charging side falls below the minimum limit set for the variable speed water pump, the mass flowrate is set to the minimum value and the temperature of the supply flow is calculated as:

$$T_{BVH,sup} = T_{BVH,ret} + \frac{\dot{Q}_{PHEX,OUT}}{c_p \cdot (\dot{m}_{BVH})_{min}} \quad (9)$$

c) Mass flowrate of discharging side:

The supply flow of the discharging side was assumed to be exiting the buffer vessel from the top layer with a temperature equal to the temperature of the top layer. Conversely, the return flow of the discharging side was assumed to be entering the buffer vessel at the bottom layer of the vessel with the design LTHW return temperature of 30 °C. Based on the supply and return flow temperatures, the discharging side mass flowrate was calculated in order to satisfy the heating demand of the store as follows:

$$\dot{m}_{BVC} = \frac{\dot{Q}_{Heating\ Demand}}{c_p \cdot (T_{BVC,sup} - T_{BVC,ret})} \quad (10)$$

d) Temperature calculation of each layer:

Based on the mass flowrates calculated for the charging and discharging sides, the temperature of each layer of the buffer vessel could be calculated at the next timestep. As an implicit finite difference method was chosen, Equation 3 can be rewritten as Equation 11 (n refers to the time, j refers to the number of layer):

$$M_j \cdot c_p \cdot \frac{T_j^{n+1} - T_j^n}{\Delta t} = \dot{m}_{BVH} \cdot c_p \cdot \left(T_{j-1}^{n+1} - T_j^{n+1}\right) + \dot{m}_{BVC} \cdot c_p \cdot \left(T_{j+1}^{n+1} - T_j^{n+1}\right)$$
$$+k \cdot A_d \cdot \frac{1}{\Delta x} \cdot \left(T_{j-1}^{n+1} - T_j^{n+1}\right) + k \cdot A_d \cdot \frac{1}{\Delta x} \cdot \left(T_{j+1}^{n+1} - T_j^{n+1}\right)$$
$$-U \cdot \frac{A_{ls}}{N} \cdot \left(T_j^{n+1} - T_{ext}\right) \quad (11)$$

This leads to the following form of equation for each layer *j*:

$$A_j \cdot T_{j-1}^{n+1} + B_j \cdot T_j^{n+1} + C_j \cdot T_{j+1}^{n+1} = -T_j^n - D_j \quad (12)$$

where:

$$A_j = \frac{\Delta t}{M_j \cdot c_p}\left(\dot{m}_{BVH} \cdot c_p + \frac{k \cdot A_d}{\Delta x}\right) \quad (13)$$

$$B_j = -1 + \frac{\Delta t}{M_j \cdot c_p}\left(-\dot{m}_{BVH} \cdot c_p - \dot{m}_{BVC} \cdot c_p - 2 \cdot \frac{k \cdot A_d}{\Delta x} - U \cdot \frac{A_{ls}}{N}\right) \quad (14)$$

$$C_j = \frac{\Delta t}{M_j \cdot c_p}\left(\dot{m}_{BVC} \cdot c_p + \frac{k \cdot A_d}{\Delta x}\right) \quad (15)$$

$$D_j = \frac{\Delta t}{M_j \cdot c_p}\left(U \cdot \frac{A_{ls}}{N} \cdot T_{ext}\right) \quad (16)$$

For the top (j=1) layer, the equation coefficients were modified as follows:

$$A_1 = \frac{\Delta t}{M_j \cdot c_p}\left(\dot{m}_{BVH} \cdot c_p\right) \quad (17)$$

$$B_1 = -1 + \frac{\Delta t}{M_j \cdot c_p}\left[-\dot{m}_{BVH} \cdot c_p - \dot{m}_{BVC} \cdot c_p - \frac{k \cdot A_d}{\Delta x} - U \cdot \left(\frac{A_{ls}}{N} + A_d\right)\right] \quad (18)$$

$$D_1 = \frac{\Delta t}{M_j \cdot c_p}\left[U \cdot \left(\frac{A_{ls}}{N} + A_d\right) \cdot T_{ext}\right] \quad (19)$$

The temperature at layer j=0 is also replaced by the temperature of the supply flow from the charging side entering the buffer vessel:

$$T_0^{n+1} = T_{BVH,sup} \quad (20)$$

For the bottom layer (j=N), the equation coefficients were modified as follows:

$$B_N = -1 + \frac{\Delta t}{M_j \cdot c_p}\left(-\dot{m}_{BVH} \cdot c_p - \dot{m}_{BVC} \cdot c_p - \frac{k \cdot A_d}{\Delta x} - U \cdot \left(\frac{A_{ls}}{N} + A_d\right)\right) \quad (21)$$

$$C_N = \frac{\Delta t}{M_j \cdot c_p}\left(\dot{m}_{BVC} \cdot c_p\right) \quad (22)$$

$$D_N = \frac{\Delta t}{M_j \cdot c_p}\left(U \cdot \left(\frac{A_{ls}}{N} + A_d\right) \cdot T_{ext}\right) \quad (23)$$

Additionally, the temperature at the layer j=N+1 is replaced by the temperature of the return flow from the discharging side entering the buffer vessel:

$$T_{N+1}^{n+1} = T_{BVC,ret} \quad (24)$$

The system of energy balance equations from each layer can then be organized in a matrix form as follows:

$$\begin{bmatrix} B_1 & C_1 & 0 & \cdots & \cdots & \cdots & \cdots & \cdots & 0 \\ A_2 & B_2 & C_2 & \ddots & & & & & \vdots \\ 0 & A_3 & B_3 & C_3 & \ddots & & & & \vdots \\ \vdots & \ddots & \ddots & \ddots & \ddots & \ddots & & & \vdots \\ \vdots & & \ddots & A_j & B_j & C_j & \ddots & & \vdots \\ \vdots & & & \ddots & \ddots & \ddots & \ddots & \ddots & \vdots \\ \vdots & & & & \ddots & A_{N-2} & B_{N-2} & C_{N-2} & 0 \\ \vdots & & & & & \ddots & A_{N-1} & B_{N-1} & C_{N-1} \\ 0 & \cdots & \cdots & \cdots & \cdots & \cdots & 0 & A_N & B_N \end{bmatrix} \begin{bmatrix} T_1^{n+1} \\ T_2^{n+1} \\ T_3^{n+1} \\ \vdots \\ T_j^{n+1} \\ \vdots \\ T_{N-2}^{n+1} \\ T_{N-1}^{n+1} \\ T_N^{n+1} \end{bmatrix} = \begin{bmatrix} -T_1^n - D_1 - A_1 \cdot T_{BVH,sup} \\ -T_2^n - D_2 \\ -T_3^n - D_3 \\ \vdots \\ -T_j^n - D_j \\ \vdots \\ -T_{N-2}^n - D_{N-2} \\ -T_{N-1}^n - D_{N-1} \\ -T_N^n - D_N - C_N \cdot T_{BVC,ret} \end{bmatrix} \quad (25)$$

2.3.4. Further considerations and assumptions

- A 10-min timestep and 10 layers for the buffer vessel discretization were chosen for the model simulations. This was a compromise between the computational time required for each full year simulation and the accuracy of the model.
- According to the thermal storage system description (Section 2.2), the desuperheater three-way valve closes when the temperature inside the buffer vessel reaches 70 °C. As this temperature limit would often be exceeded because of the 10-min timestep, a limit of 67.5 °C was adopted for the simulations.
- The operating pressure and maximum design temperature of the buffer vessel were assumed to be 3 bar and 99 °C respectively based on the buffer vessel specification obtained from The Biomass Hut (2019).
- The mass of the water inside the vessel was considered as constant throughout the one-year simulation. It was calculated as a function of the volume of the vessel and the density of water at the operating pressure and maximum design temperature.
- The buffer vessel was assumed to be always completely filled with water, i.e., there was equal mass of water at each layer.
- The overall heat transfer coefficient of the buffer vessel (U) was assumed to be 0.22 W m^{-2} K^{-1} based on information provided by Mibec (2019).
- As the heat is transferred to the vessel by two identical charging side circuits, the heating demand requirements are assumed to be equally divided between the two circuits. As mentioned in Section 2.2, the minimum setting of the variable speed water pump is 10% of the maximum flowrate during operation. As the total maximum flowrate required for the charging side was approximately 3 kg/s during operation, the minimum flowrate was defined as: $(\dot{m}_{BVH})_{min} = 0.3\ kg/s\ (or\ 0.15\ kg/s\ for\ each\ charging\ side\ circuit)$
- According to Lamb (2018), the compressors account for 80-90% of the electricity consumption of a refrigeration system while the condensers and evaporators account for 10-20%. Thus, it was assumed that the electricity consumption was exclusively due to the compressors while the energy consumption of condensers, evaporators, gas coolers.
- Based on discussions with industry, the auxiliary energy consumption by the circulating water pumps is minimal compared to the overall energy consumption of the CO_2 supermarket refrigeration systems. As all system configurations discussed in the following section require circulating pumps, the energy consumption of the circulating pumps was neglected as it would not have a significant impact on the comparisons.
- The return temperature of the CO_2 refrigerant from the LTHW desuperheater was assumed to be 45 °C based on consultation with industry. Although a lower return temperature would increase the amount of recoverable

heat, a desuperheater with larger heat transfer area would be required which would both be more expensive and require more installation space.

- The thermal properties of the water inside the buffer vessel were assumed to be constant and were calculated based on a temperature of 50 °C and the operating pressure of 3 bar.
- This study focuses only on the operational performance of the RIHC systems with thermal storage. The capital costs associated with these systems were not considered as part of this study.

3. Case Study and Scenario Descriptions

3.1. Simulation strategies

The annual performance of a baseline scenario and five additional control strategies were simulated. It should be noted that the provision of adequate cooling to the MT and LT cabinets remains the priority for all the control strategies simulated.

3.1.1. Baseline Case: Business as usual

The cooling to the food cabinets and the space heating are provided by two independent systems. The cooling is provided by the CO_2 booster refrigeration system operating at floating condensing conditions. A gas boiler system provides the space heating demand to the store. The refrigeration system is responsible for the electricity consumption and the gas boiler for the gas consumption. No heat is recovered. A boiler efficiency of 93% was assumed consistent with Sarabia Escriva et al. (2019). This scenario depicts how conventional heating and refrigeration systems perform in supermarket buildings.

3.1.2. Case 1: Heat recovery with a gas boiler system

The refrigeration system operates at a floating condensing conditions similarly to the Baseline. In this case, however, heat is recovered from the refrigeration system by the desuperheater and is used to provide the space heating. If the space heating demand exceeds the recoverable heat, a gas boiler is used to supplement the remainder of the demand. This scenario examines the effect of adding a desuperheater to recover a portion of the heat rejected by the refrigeration system on the performance of the baseline case.

3.1.3. Case 2: RIHC system without thermal storage

The refrigeration system is responsible for the provision of both the space heating to the store and the cooling to the LT and MT cabinets. The space heating is provided directly from the desuperheater of the refrigeration system eliminating the need for a gas boiler. If the recoverable heat from the system exceeds the heating demand, the system operates at a floating condensing pressure similarly to Case 1. Otherwise, the measures described in Section 2.1.3 are taken in order to increase the amount of recoverable heat. The upper limit of the

condenser pressure for heat recovery is fixed at 100 bar. This case examines whether the space heating to the store can be provided exclusively by the refrigeration system eliminating the need for a gas boiler.

3.1.4. Case 3: RIHC system with thermal storage

A thermal storage system is integrated into the RIHC system of Case 2 as described in Section 2.2. The heat recovered from the refrigeration system is used to maintain the water at the top of the buffer vessel at a temperature of at least 45 °C instead of directly being used for space heating. If the recoverable heat is not sufficient to maintain the required temperature, the measures for additional heat recovery described in Section 2.1.3 are applied to increase the amount of recoverable heat. If the buffer vessel temperature exceeds 70 °C, the desuperheater three-way valve is closed and no heat is transferred to the vessel. The maximum condenser pressure limit for heat recovery is fixed at 100 bar. In this case, the effect of incorporating a thermal storage system on the performance of a RIHC system is studied.

3.1.5. Case 4: RIHC system with thermal storage and a floating maximum condenser pressure limit for heat recovery

The operational strategy is similar to Case 3. In this case, the least amount of electricity consumption is obtained for each timestep by iterating through different values of maximum condenser pressure for heat recovery between 80 and 100 bar. Thus, the optimal maximum condenser pressure for heat recovery can be determined for a RIHC system with thermal storage by examining this scenario.

3.1.6. Case 5: RIHC system with thermal storage modified for additional heat accumulation in the buffer vessel during winter weekdays

The operational strategy is similar to Case 3. However, it is modified between the colder months from September to April, Monday to Friday, 07:30-16:00 in order to reduce the peak recoverable heat requirements from the refrigeration system by accumulating more heat inside the vessel during the day. This is achieved by increasing the condenser pressure to the maximum allowable limit (even when the buffer vessel can be maintained at 45 °C with a lower condenser pressure) if the following conditions are valid:

- The temperature at the top of the buffer vessel is below 62.5 °C between 07:30 and 08:00.
- The temperature at the top of the buffer vessel is below 55 °C between 08:00 and 16:00.

A fixed maximum condenser pressure of 100 bar was adopted for heat recovery. This case was considered in order to examine whether the performance of the RIHC system with thermal storage described in Case 3 could be further improved by adopting an alternative control strategy during the colder periods of the year.

3.2. Case study description

Consistent with the work of Sarabia Escriva et al. (2019), simulations were carried out by using data obtained from a supermarket store located in the West Midlands region of the UK. The store first opened in 2015 with opening hours

from 08:00 to 21:00 between Monday and Saturday and from 10:00 to 16:00 on Sunday. It has a total sales area of 1,600 m^2 which is maintained at a temperature of 19 °C during the opening hours and 16 °C when the store is closed.

The simulations were carried out for the one-year period between September 2017 and August 2018. The heating demand data of the store was obtained from half-hourly metered data available in an energy management database. The heating demand profiles for a typical summer and winter week are illustrated in Figure 6. It can be observed that the heating demand spikes at 08:00 of each weekday. This is because the temperature set point is lowered to 16 °C during the night and thus, a substantial amount of heating is required to raise the temperature to 19 °C as quickly as possible when the store opens.

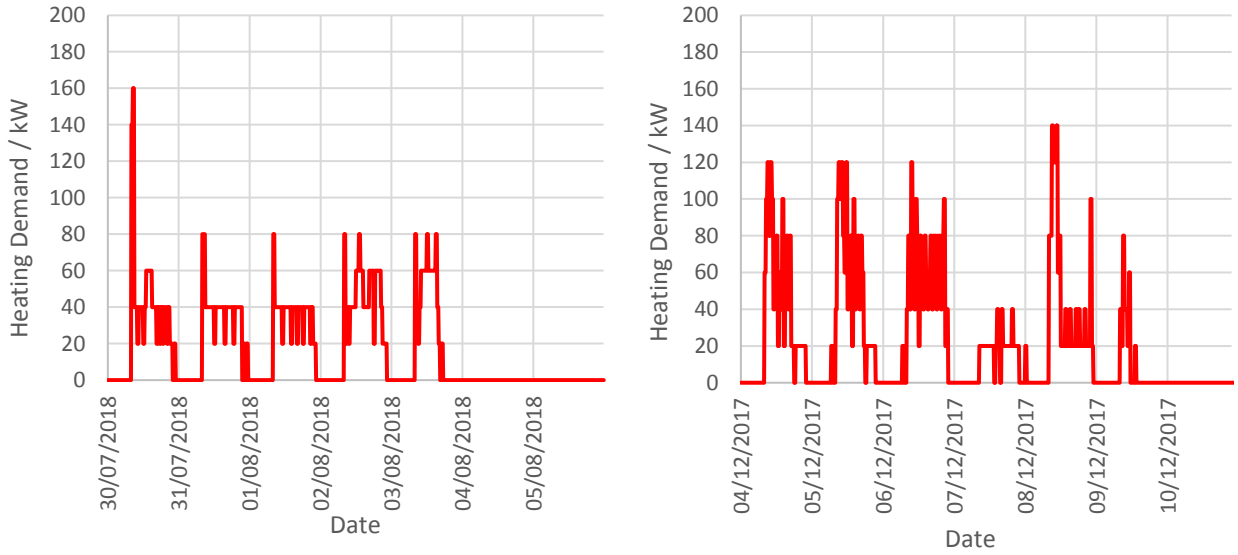

Figure 6. Half-hourly heating demand profiles for a typical summer week (left) and winter week (right).

The half-hourly electricity prices for the DNO region of the store under consideration between September 2017 and August 2018 were provided by industry partners. These prices were subsequently inflated to reflect the 2018-2019 prices based on the percentage that the average electricity price increased between the two time periods. The price of natural gas was assumed to be constant at 3 p/kWh throughout the year (BEIS, 2019). The GHG emissions factors for electricity and natural gas were adopted as 0.2556 kg CO_{2e} and 0.1838 kg CO_{2e} respectively (UK Government, 2019).

The weather data used for the simulations were obtained from the online weather database Dark Sky API (2019) for the location of the store. The specification of the buffer vessels was obtained from The Biomass Hut (2019).

4. Results and Discussion

4.1. Key results

The results obtained from the simulations are summarized in Table 1 in terms of annual operating costs, GHG emissions and energy consumption:

Table 1. Summary of results in terms of annual operating costs, GHG emissions and energy consumption.

	Baseline Case	**Case 1**	**Case 2**	**Case 3**	**Case 4**	**Case 5**
Electricity cost (£)	30,380	30,380	34,999	34,203	34,214	34,246
Gas cost (£)	5,026	3,060	0	0	0	0
Annual operating costs (£)	35,406	33,440	34,999	34,203	34,214	34,246
Electricity emissions (tCO_{2e})	66.0	66.0	75.2	73.4	73.3	73.9
Gas emissions (tCO_{2e})	30.6	18.6	0.0	0.0	0.0	0.0
Annual GHG emissions (tCO_{2e})	96.6	84.6	75.2	73.4	73.3	73.9
Electricity consumption (MWh)	260.3	260.3	296.4	289.5	289.6	291.3
Gas consumption (MWh)	166.0	94.0	0.0	0.0	0.0	0.0
Annual energy consumption (MWh)	426.3	354.3	296.4	289.5	289.6	291.3

As indicated in Table 1, the variations in operating costs between the five cases appear are small as the annual operating costs include both the costs of refrigeration and heating. However, more than 80% of the operating costs are associated with the minimum requirements for refrigeration. Thus, the effect of the control strategies used in each case appear to be identical because they affect the cost for heating which is only a small fraction of the total annual operating costs. On the other hand, as the space heating provision is responsible for a larger portion of the overall GHG emissions and primary energy use, the effect of RIHC systems with thermal storage is significant compared to conventional gas boiler solutions.

The most cost-effective control strategy is Case 1 for which the gas boiler is used to supplement the difference between the heating demand and the recoverable heat from the refrigeration system. The adoption of Case 1 leads to annual savings in operating costs by 2.2% compared to the RIHC system with thermal storage in Case 3, the second most cost-effective case. Although Case 1 is the most cost-effective strategy, it is outperformed by Case 3 in terms of annual GHG emissions and energy consumption by 13.2% and 18.2% respectively. This is due to the fact that the use of the gas boiler in Case 1 leads to a higher annual energy consumption compared to Cases 2-5 for which the heating is provided exclusively by the refrigeration system. Despite the additional annual energy consumption, Case 1 is the most cost-effective solution as the average price of gas is approximately 25-30% of the average electricity price.

For cases 2-5, the refrigeration system is responsible to provide both the space heating to the store and the cooling to the chilled and frozen food cabinets. Among these cases, the integration of a buffer vessel into the system (Cases 3-5) leads to a decrease of the annual operating costs by at least 2.2% compared to Case 2 for which the heating is provided directly from the desuperheater. This is because the buffer vessel enables the storage of the heat recovered during periods with excess amount of recoverable heat.

Among the cases with thermal storage (Cases 3-5), Case 3 yields the lowest annual operating costs. It slightly outperforms Case 4 which involves a more complex control strategy with a floating maximum condenser pressure for heat recovery. Between the two cases using a fixed maximum pressure limit for heat recovery, Case 3 outperforms Case 5 in terms of annual operating costs by 0.3%. However, Case 5 represents a more realistic depiction of the annual operating costs. This is because the margin of 16% compared to the maximum HP compressor capacity obtained for Case 5 would be more likely to be adopted in practice than the 6% obtained for Case 3 (Table 2). Compared to Case 1, the implementation of Case 5 would result in an increase of annual operating costs by 3.2% and a decrease of annual GHG emissions and energy demand by 12.7% and 17.8% respectively.

Table 2. Results of compressor capacity required and volume of buffer vessel for each case scenario.

	Baseline Case	**Case 1**	**Case 2**	**Case 3**	**Case 4**	**Case 5**
Maximum HP compressor capacity required (%)	54.4	54.4	71.6	93.9	93.9	84.2
Buffer vessel volume (m^3)	-	-	-	2	2	2.5

4.2. Analysis of Case 1: Heat recovery with a gas boiler system

In this case, the refrigeration system operates at a floating condensing pressure (similar to the Baseline case) with the additional benefit of heat recovery. This leads to a decrease of the annual gas demand and thus, a reduction of the annual gas and operating costs by 39.1% and 5.6% respectively. The decrease of gas demand also leads to a reduction of the total GHG emissions by 12.4%. The extra heat recovered compared to the heating demand cannot be exploited with this strategy.

The profile of heating demand, recoverable heat and gas consumption for a typical summer weekday is demonstrated in Figure 7. As shown in the figure, the gas boiler would be required only between 08:00-08:30 when the store opens and the heating demand reaches its peak value. For the remainder of the day, the recoverable heat from the refrigeration system is sufficient to provide the space heating to the store.

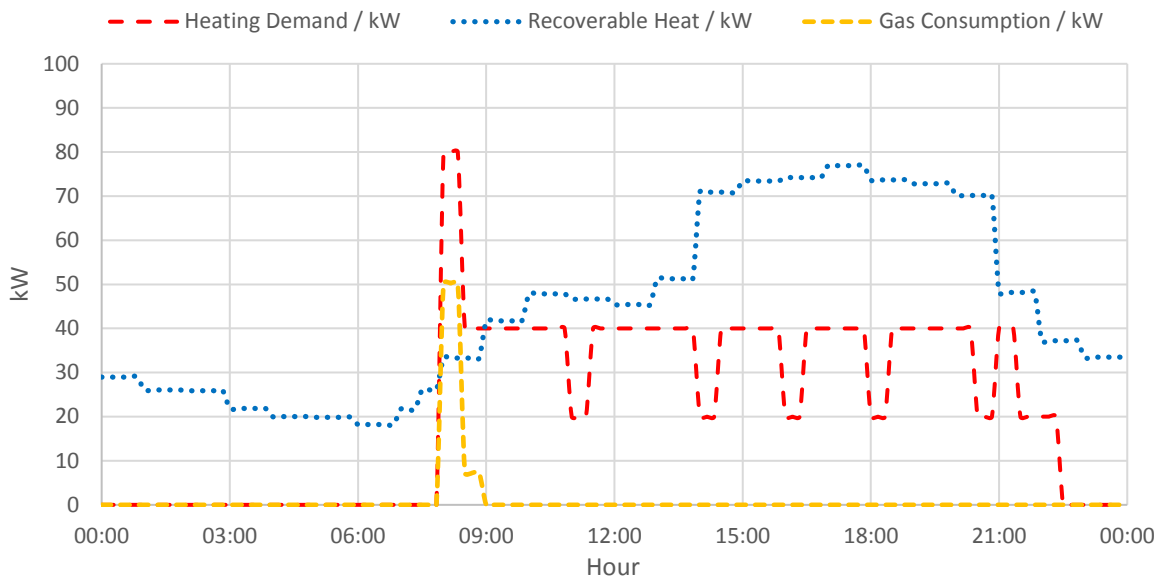

Figure 7. Profiles for heating demand, recoverable heat and gas consumption for Case 1 during a typical summer weekday (01/08/2018).

Figure 8 illustrates the same profiles for a typical winter weekday. It can be observed that the recoverable heat from the refrigeration system is reduced compared to a typical summer weekday. This is caused by the reduced cooling load to the refrigeration system due to the lower exterior temperatures in the winter. Thus, the majority of the space heating during the store's opening hours is provided by the gas boiler. The heat recovered from the refrigeration system during the opening hours is used to reduce the gas consumption.

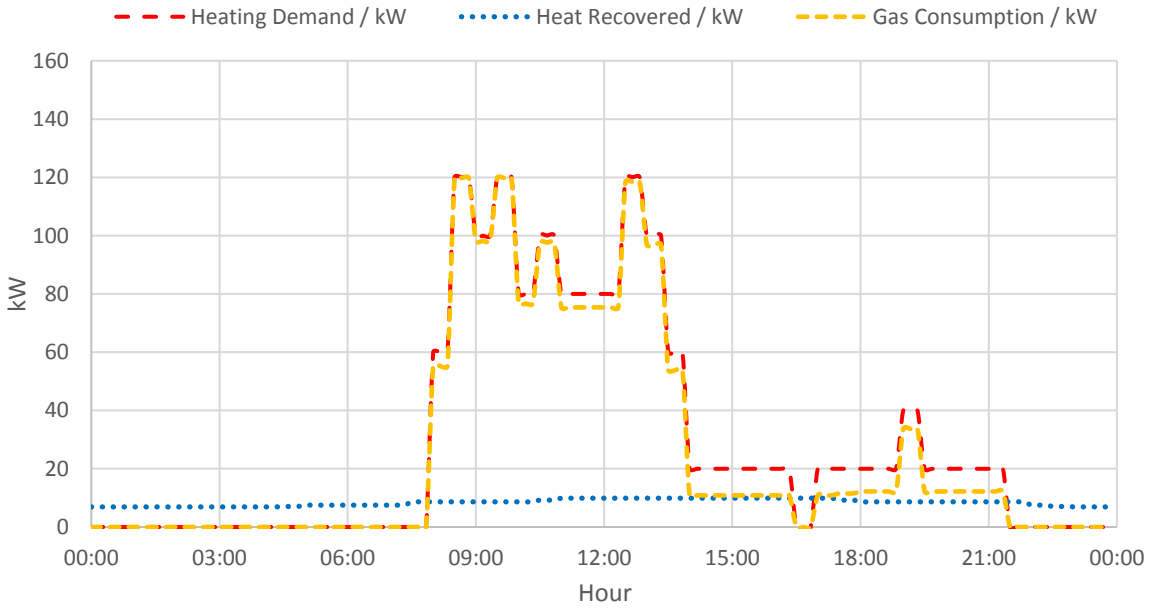

Figure 8. Profiles for heating demand, recoverable heat and gas consumption for Case 1 during a typical winter weekday (27/12/2017).

4.3. Analysis of Case 2: RIHC system without thermal storage

The RIHC system without thermal storage of Case 2 requires the refrigeration system to provide both the space heating demand to the store and the cooling to the chilled and frozen food cabinets. This is achieved by increasing the amount of recoverable heat using the measures described in Section 2.1.3. Similar to Case 1, the additional amount of recoverable heat compared to the heating demand is not exploited.

The profiles of heating demand, recoverable heat and condenser pressure for a typical summer obtained for Case 2 are displayed in Figure 9. The recoverable heat follows a similar path to the equivalent summer weekday using the Case 1 strategy as it operates at a floating condenser pressure (Figure 9). At the store opening time, however, the recoverable heat at floating condenser pressure conditions is less than the heating demand (Figure 7). Thus, there is an increase of the condenser pressure which reflects the peak of heating demand (Figure 9). This leads to an increase of the recoverable heat which matches the heating demand eliminating the need for a gas boiler.

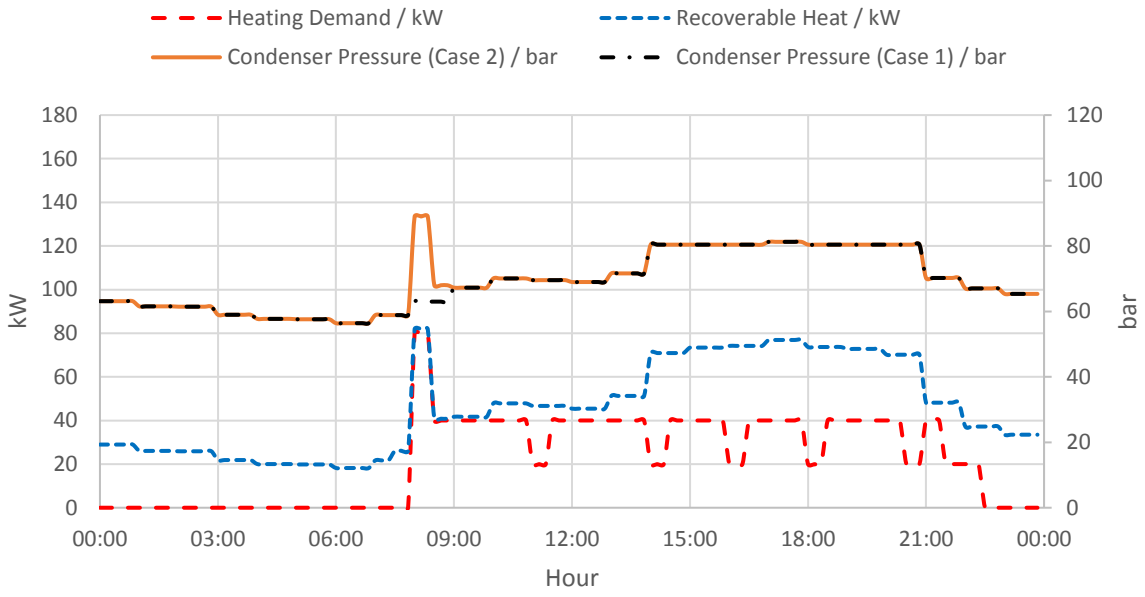

Figure 9. Profiles for heating demand, recoverable heat and condenser pressure for Case 2 during a typical summer weekday (01/08/2018).

During the store opening hours in a winter weekday, the heating demand exceeds the amount of heat that can be recovered when the refrigeration system operates at a floating condenser pressure (Figure 8). Thus, the recoverable heat is increased by raising the condenser pressure which results in a condenser pressure profile which reflects the heating demand profile during the store opening times (Figure 10).

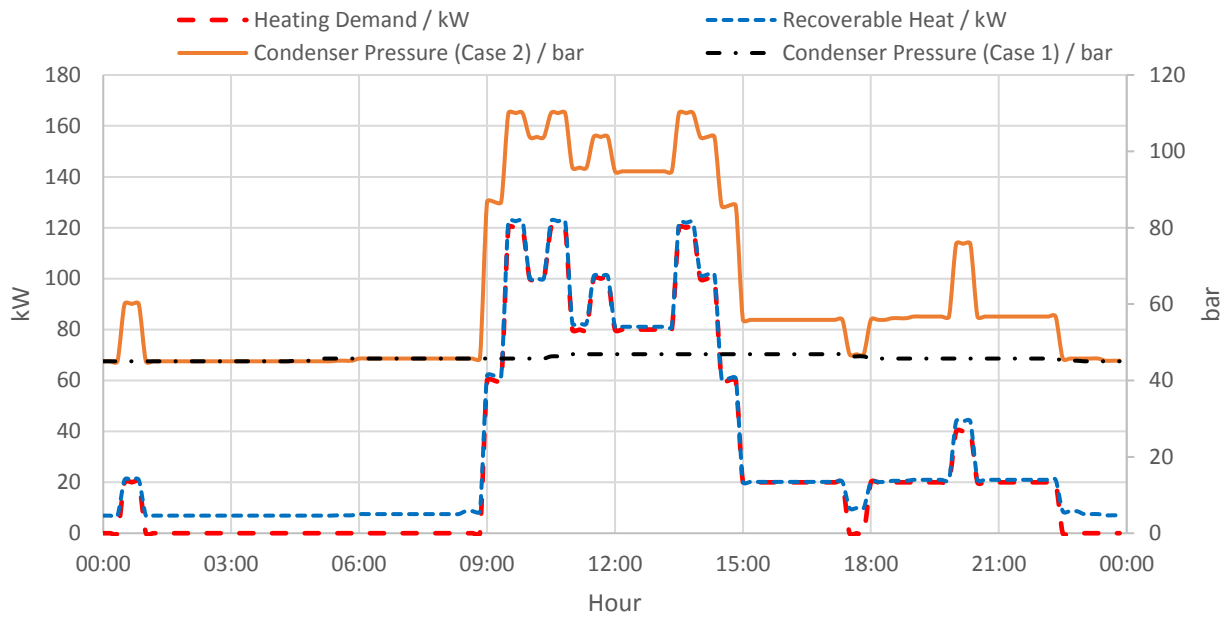

Figure 10. Profiles for heating demand, recoverable heat and condenser pressure for Case 2 during a typical winter weekday (27/12/2017).

Although the control strategy described in Case 2 is theoretically feasible, it has been proven difficult to commission in practice based on discussions with industry. This is because the refrigeration system could not instantaneously react to the fluctuating heating demand by raising the pressure of the condenser and reducing the gas cooler fan speed. These issues led to under-heating because of the fluctuations of the water temperature of the LTHW space heating supply flow.

4.4. Analysis of Case 3: RIHC system with thermal storage

This system is referred to as a RIHC system with thermal storage as it involves the integration of a buffer vessel into the system. This strategy aims to always maintain the temperature at the top of the buffer vessel above 45 °C. This enables the system to maintain the necessary quality of heat through temperature stratification inside the vessel which smooths out the fluctuations caused by the varying heating demand. Thus, the practical problems that Case 2 faces are reduced by the integration of the buffer vessel. In addition, the buffer vessel is used as a thermal storage device when there is an excess amount of recoverable heat leading to a reduction of the annual operating costs.

The size of the buffer vessel selected for Case 3 was selected as 2 m^3 and it required an HP compressor capacity of 93.9% compared to the capacity installed in the store (Table 2). The selection of a larger buffer vessel (2.5 m^3) would reduce the annual operating costs as it would allow a larger amount of heat to be stored during low heating demand periods. However, it would also lead to an increase of the maximum HP compressor requirements to 103.1% as more heat would be required to maintain the vessel at 45 °C during peak heating demand periods due to the additional water inside the vessel. As the installation of additional HP compressor

capacity would lead to a significant increase of the system's capital cost, the following analysis will be focused on the results obtained with a buffer vessel of 2 m^3.

Alternatively, the concerns regarding the HP compressor capacity problem of the RIHC system with thermal storage studied in Case 3 could be potentially alleviated by maintaining the store at 19 °C during the night instead of 16 °C. The main benefit from this change would be the reduction of the peak heating demands at the store opening time. Additionally, the cooling demand of the food cabinets during the night would increase and therefore, more heat would be stored in the buffer vessel as it is recovered from the refrigeration system. However, this approach which would allow a use of a larger buffer vessel than 2 m^3 is outside the scope of this research as a detailed model would be required to simulate how the change of the heating demand strategy would affect the heating demand profile.

Figure 11 depicts the profiles of heating demand, recoverable heat and the temperature at the top of the buffer vessel during a typical summer weekday for Case 3. The temperature profile of the buffer vessel before the opening hours involves alternating peaks and troughs between 67.5 °C and 73 °C. The troughs are caused by the assumption made for the model that the desuperheater three-way valve closes and no heat is transferred to the vessel when its temperature exceeds 67.5 °C. The amplitude of the fluctuations can be explained by the 10 mins timestep used for the simulations which leads to a delayed reaction from the model in terms of closing the desuperheater valve. As explained in Section 2.3.4, this delayed response from the model was the reason that led to using a 67.5 °C temperature limit for the buffer vessel instead of 70 °C.

The heat stored in the buffer vessel allows the system to maintain the floating condensing pressure when the heating demand spikes at the store opening time. Subsequently, the recoverable heat exceeds the heating demand and thus, the buffer vessel is recharged to a temperature of approximately 67.5 °C.

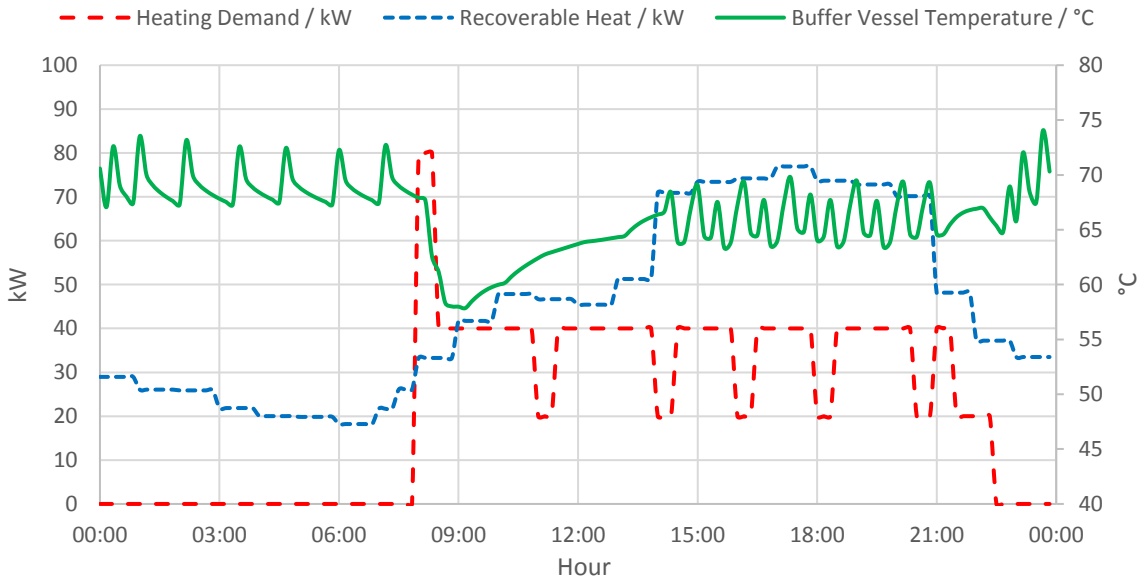

Figure 11. Profiles for heating demand, recoverable heat and temperature at the top of the buffer vessel for Case 3 (2 m^3) during a typical summer weekday (01/08/2018).

During a typical winter weekday, the cooling load to the refrigeration system is lower during the night compared to a summer weekday as the exterior temperatures are lower. Thus, less heat can be recovered from the refrigeration system and the buffer vessel cannot be fully charged before the store opens (Figure 12). Combined with the higher peak heating demand compared to a summer weekday, the buffer vessel quickly discharges approximately 50 minutes after the store opening. The amount of recoverable heat should match and even slightly exceed the heating demand for the remainder of the day so that the top of the buffer vessel is maintained at a temperature of 45 °C.

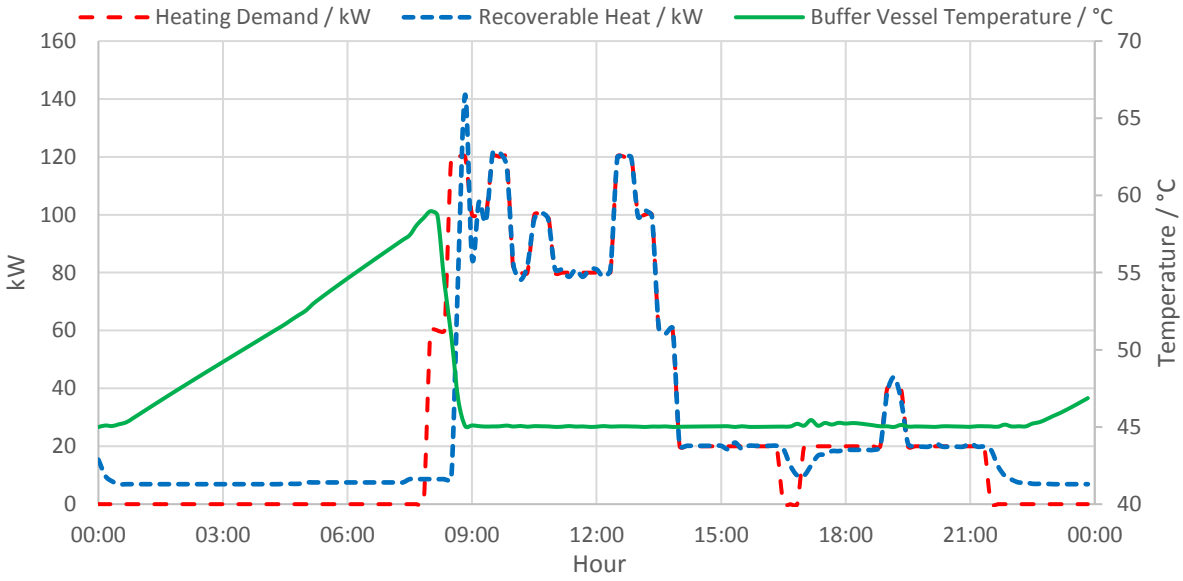

Figure 12. Profiles for heating demand, recoverable heat and temperature at the top of the buffer vessel for Case 3 (2 m^3) during a typical winter weekday (27/12/2017).

The first measure taken to increase the recoverable heat to maintain the top of the buffer vessel above 45 °C is to raise the condenser pressure (Figure 13). If the condenser pressure is raised to the maximum allowable limit (100 bar) and the recoverable heat is still insufficient, the gas cooler fan speed is reduced leading to an increase of the gas cooler outlet temperature (Figure 13). For the winter weekday depicted in Figure 13, the gas cooler outlet temperature was not required to be raised at 45 °C and thus, the false load evaporator was not employed for additional heat recovery.

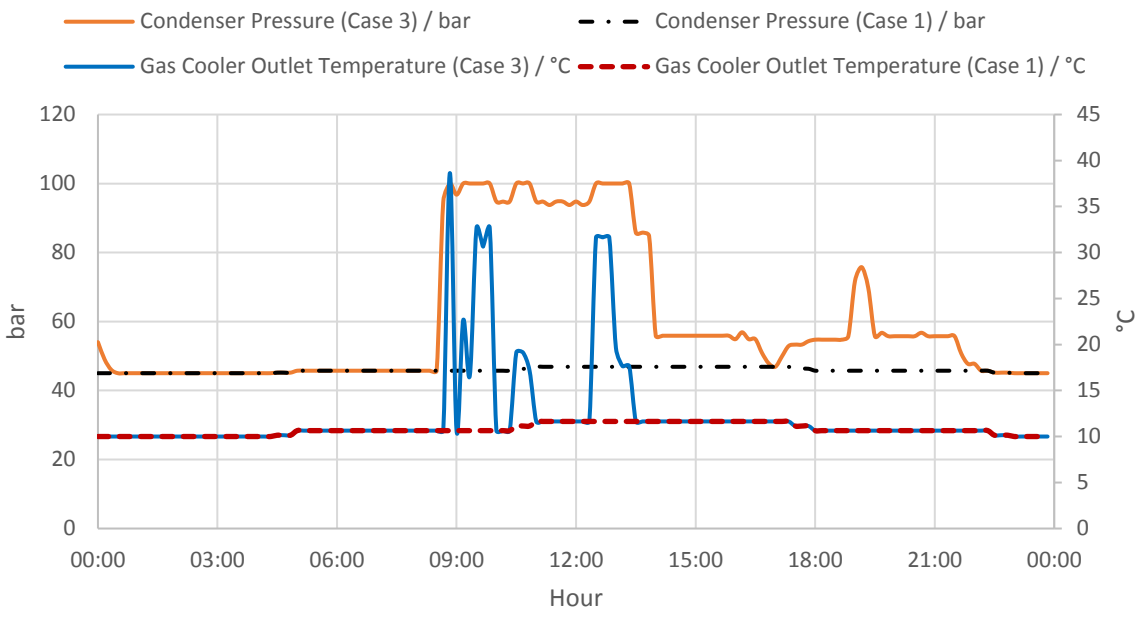

Figure 13. Profiles for condenser pressure and gas cooler outlet temperature for Case 1 and Case 3 (2 m^3) during a typical winter weekday (27/12/2017).

4.5. Analysis of Case 4: RIHC system with thermal storage and a floating maximum condenser pressure limit for heat recovery

In Case 4, the RIHC system with thermal storage was considered to be operating at a floating maximum condenser pressure for additional heat recovery between 80 and 100 bar in order to minimize the electricity consumption at each timestep.

The results (Table 1) suggest that the Case 4 strategy leads to a decline of the system performance compared to Case 3. This decline is translated to a 0.03% increase in annual operating costs and GHG emissions. As Case 4 requires both a more complex control strategy and it also leads to a slight decline in performance, it does not present a viable alternative to Case 3.

As illustrated in Figure 14, the pressure profile of Case 4 is similar to the pressure profile of Case 3. This suggests that the performance of the RIHC with thermal storage system is optimized when it operates with a fixed maximum condenser pressure limit for heat recovery of 100 bar, i.e., the maximum pressure limit allowed in practice.

The slight decline in performance obtained in Case 4 can be explained by the fact that minimizing the electricity consumption at each timestep is also translated to minimum heat input to the buffer vessel. Thus, during peak heating demand hours, the heat accumulated in the buffer vessel was slightly more in Case 3 than Case 4 reducing the peak recoverable heat requirements. As the deterioration of the refrigeration system's COP is proportional to the peak of the recoverable heat requirements, the slight reduction of peak recoverable heat requirements in Case 3 leads to a slightly better annual performance.

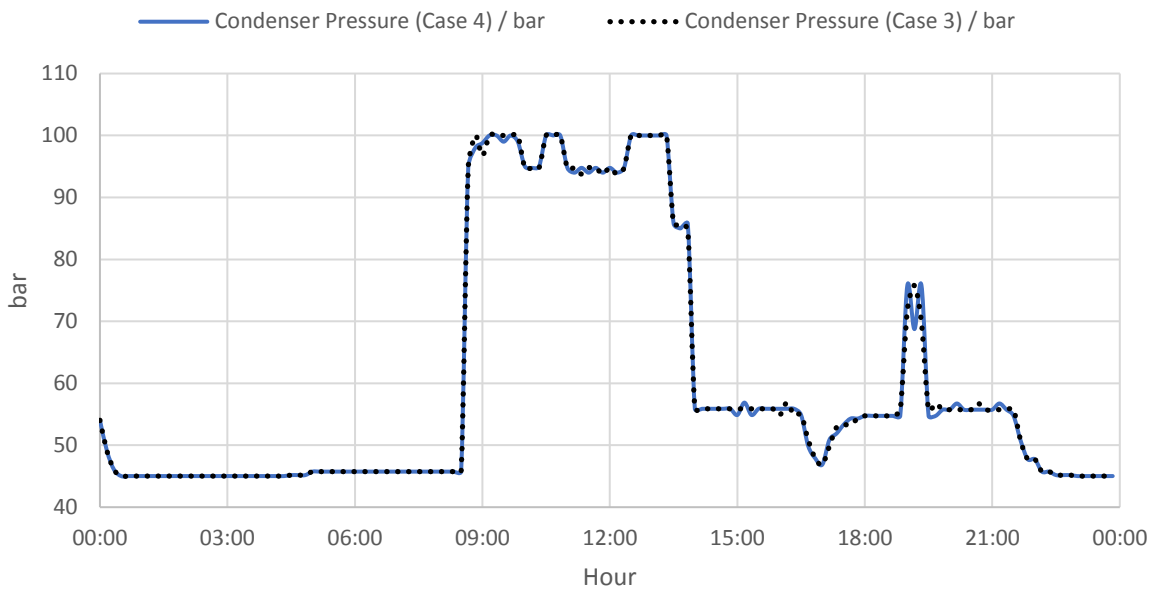

Figure 14. Profiles for condenser pressure for Case 3 (2 m^3) and Case 4 (2 m^3) during a typical winter weekday (27/12/2017).

4.6. Analysis of Case 5: RIHC system with thermal storage modified for additional heat accumulation in the buffer vessel during winter weekdays

In addition to maintaining the top of the buffer vessel at a temperature of at least 45 °C, this control strategy aims to accumulate extra heat inside the vessel and thus, prevent the vessel from completely discharging between September and April. This is achieved by raising the condenser pressure to the maximum limit if either the temperature at the top of the buffer vessel is below 62.5 °C between 07:30 and 08:00 or the temperature falls below 55 °C between 10:00 and 16:00.

As noted in Section 2.4.6, the maximum condenser pressure limit is fixed at 100 bar. Using the Case 5 strategy, the system can be employed with a 100-bar pressure limit and a 2.5 m^3 buffer vessel without the requirement for additional HP compressor capacity. This is because the maximum HP compressor capacity requirement is reduced to 84.2% of the existing installed capacity (Table 2) compared to the 103.1% capacity required for Case 3 with the same buffer vessel size.

As the Case 5 control strategy is identical to Case 3 during the summer, the following analysis will focus on the differences during a typical winter weekday. As shown in Figure 15, the first change in system behaviour between the two cases can be observed at 07:30, thirty minutes before the store opening. At that point, the temperature at the top of the buffer vessel in Case 5 is raised to 66 °C compared to the 55 °C in Case 3. As shown in Figure 16, this is achieved by raising the condenser pressure to the maximum allowable limit.

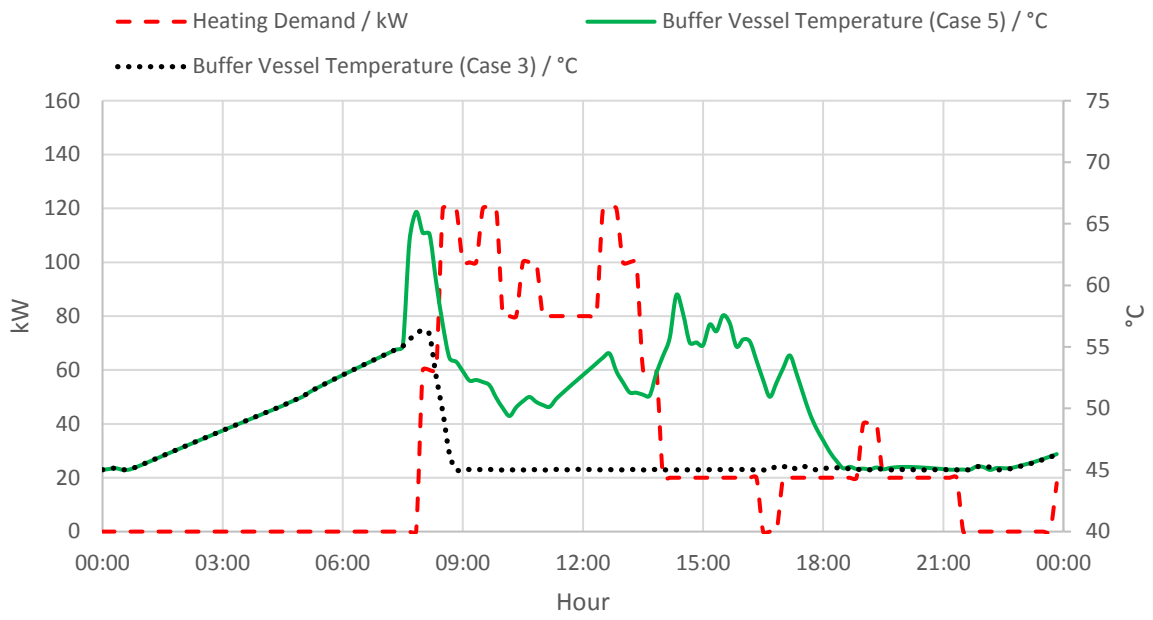

Figure 15. Profiles for heating demand, recoverable heat and temperature at the top of the buffer vessel for Case 3 (2.5 m^3) and Case 5 (2.5 m^3) during a typical winter weekday (27/12/2017).

After the store opening at 08:00, it can be observed that in Case 3, the temperature of the buffer vessel is maintained at the minimum limit of 45 °C whereas in Case 5, it is maintained higher than 45 °C (Figure 15). This is achieved by keeping the condenser pressure at the maximum allowable limit (100 bar) provided that the temperature at the top of the buffer vessel is below 55 °C (Figure 16). The effect of maintaining a higher buffer vessel temperature (i.e., having a larger amount of heat stored in the buffer vessel throughout the day) can be observed in Figure 16 between the 09:00 and 14:00. During that period, reducing the gas cooler fan speed is not required in Case 5 and thus, the gas cooler outlet temperature is maintained at the minimum amount. In Case 3, as no extra heat was previously accumulated in the buffer vessel, the gas cooler outlet temperature is raised above the minimum limit for five intervals (Figure 16).

After 16:00, Case 5 no longer involves the accumulation of heat in addition to the amount required to keep the temperature of the buffer vessel above 45 °C. This enables the system to avoid extra electricity consumption during the peak period of electricity prices in winter between 16:00 and 19:00. It also allows the system to fully discharge before the store closes so that the recoverable heat during the night can be exploited. There also lies a large area of improvement for Case 5 as the buffer vessel was not fully discharged during some days. Thus, less amount of 'free' heating was used during the night and was instead paid for during the previous day resulting in the 0.3 % increase in annual operational costs compared to Case 3 with a 2 m^3 buffer vessel.

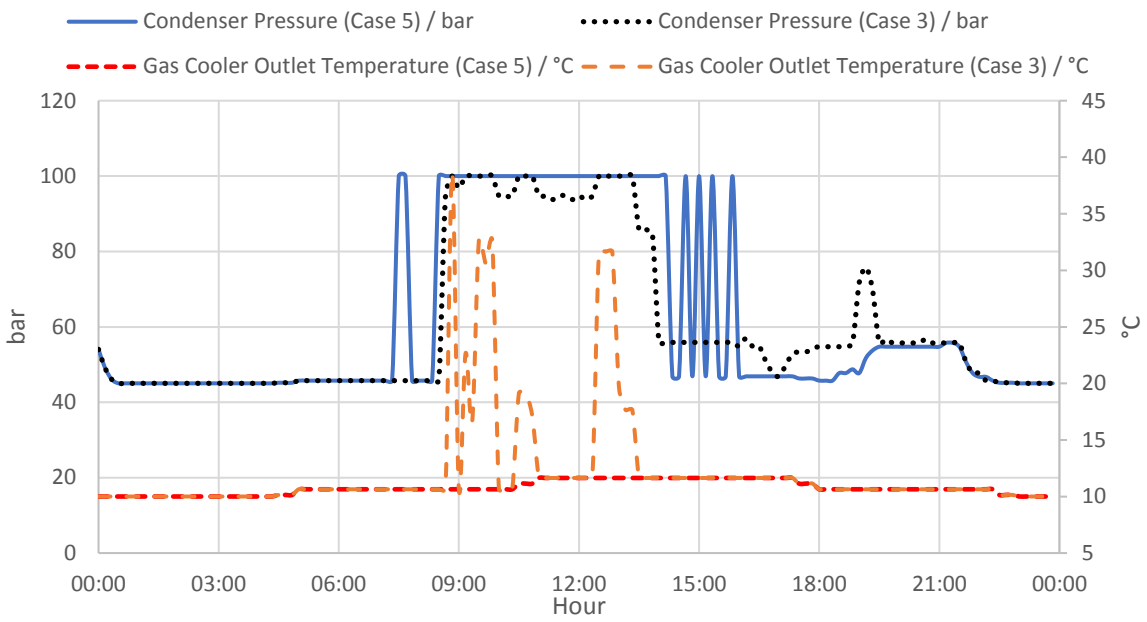

Figure 16. Profiles for condenser pressure and gas cooler outlet temperature for Case 3 (2.5 m^3) and Case 5 (2.5 m^3) during a typical winter weekday (27/12/2017).

4.7. Analysis of system behaviour

The refrigeration system in Cases 2-5 is required to provide both the space heating and the cooling to the cabinets and thus, a larger amount of heat is produced and then recovered from the refrigeration system. This is reflected in Table 3 which shows an increase of the recoverable heat to heating demand ratio for cases 2-5 compared to Case 1. However, the RIHC systems (Cases 2-5) use a larger percentage of the recoverable heat compared to Case 1 leading to the decrease of energy consumption as discussed in Section 3.1. The integration of thermal storage in cases 3-5 magnifies this effect as it enables the system to exploit the excess amount of recoverable heat during low heating demand periods.

Table 3. Results of performance indicators and system behaviour for the simulated cases.

	Case 1	**Case 2**	**Case 3**	**Case 4**	**Case 5**
Ratio of recoverable heat to heating demand (%)	146.0	204.6	192.0	192.0	198.9
Ratio of useful heat recovered to recoverable heat (%)	29.7	48.9	61.2	61.2	62.4
COP	3.81	3.21	3.30	3.30	3.31
Time of transcritical operation (hours)	578	1,775	1,514	1,514	1,570

The coefficient of performance can be calculated using Equation 25 as a function of the heat absorbed from the IT and LT evaporators, the useful heat recovered and the electricity consumption. As indicated in Table 3,

Case 1 has the highest coefficient of performance. This was expected as the system in Case 1 always operates at the optimal condensing pressure. Conversely, the performance of the RIHC systems in cases 2-5 is sacrificed on many occasions so that the necessary heat can be recovered to directly satisfy the heating demand or maintain the buffer vessel at 45 °C.

$$COP = \frac{\dot{Q}_{HR,useful} + \dot{Q}_{LT,evap} + \dot{Q}_{MT,evap}}{\dot{W}_{LP} + \dot{W}_{HP}} \quad (25)$$

Another major difference between the operation of the CO_2 refrigeration system in Case 1 is that it operates in transcritical conditions approximately three times less compared to the RIHC system (Cases 2-5) as indicated in Table 3. The RIHC system without thermal storage in Case 2 operates the most hours in transcritical model as the absence of thermal storage means that it has to instantaneously react to every heating demand fluctuation. The majority of those extra transcritical hours occur during the winter when the heating demand is higher. Thus, the effect of the extra hours of transcritical operation on the performance and degradation rate of the refrigeration equipment should be carefully examined before opting for the use of RIHC systems.

4.8. Limitations and validity of the model

The one-dimensional thermal storage model described in this paper was integrated into the steady-state model developed by Sarabia et al. (2019). As a timestep often minutes was chosen, the steady-state nature of the model means that the model takes a snapshot of the thermodynamic conditions every ten minutes. In practice, however, the thermodynamic properties are constantly changing. Additionally, the steady state nature of the model did not allow the incorporation of dynamic factors such as the speed at which the refrigeration system can adjust its high-side pressure which has been neglected for the purposes of this study. Despite that, the model developed by Sarabia et al. (2019) had an error of less than 10% in instant power input and less than 1% in annual energy consumption.

The lack of experimental data availability from an actual RIHC with thermal storage installation prevented the experimental calibration of the one-dimensional thermal storage model developed as part of this study. However, the validity of the one-dimensional thermal storage model developed is supported by the energy balance equation used to calculate the temperature of each layer of the buffer vessel, which was obtained from Raccanello, Rech & Lazzaretto (2019). The simulations carried out by Raccanello, Rech & Lazzaretto (2019) using a one-dimensional model with a similar buffer tank configuration showed that the temperatures of each layer of the tank were all calculated within a 5% error compared to the experimental data. Another study for thermal energy storage in a water storage tank carried out by Nash, Badithela & Jain (2017) showed a root square mean error of 0.1 compared to experimentally obtained data using a model with 10 nodes, similar to the model developed as part of this study. Additionally, a de-stratification conductivity (k_{destr}) coefficient of 0.285 $m^{-1}K^{-1}$ was incorporated in the thermal storage model to improve its accuracy. This value was adopted based on the

work carried out by Angrisani et al. (2014) who developed and calibrated a one-dimensional thermal storage model using experimental data.

A limited amount of research has been published associated with the incorporation of thermal storage using water as a medium to CO_2 booster refrigeration systems. Other studies focused on heat recovery from CO_2 refrigeration systems to district heating (Raka Adrianto, Grandjean & Sawalha, 2018) or integration of geothermal storage to CO_2 refrigeration systems (Mateu-Royo *et al.*, 2018). Two studies that used a similar configuration were carried out by Noding et al. (2016) and D'Agaro, Coppola & Cortella (2019). The model developed by Noding et al. (2016) aimed to maintain the tank temperature above 32 °C compared to the 45 °C adopted for the model of this paper based on the HVAC system requirements of the supermarket used as a case study.

A minimum of 45 °C temperature supply for the space heating buffer tank was also adopted in the model developed by D'Agaro, Coppola & Cortella (2019) based on an actual all-in-one CO_2 booster installation in northern Italy which is integrated with thermal storage tanks for both the supply of space heating and hot water. The model by D'Agaro, Coppola & Cortella (2019) was based on a CO_2 booster refrigeration system with parallel compression which has been proven more energy efficient than the standard booster system in countries with mild to warm climates (Gullo et al., 2017). Conversely, the model developed as part of this study was based on a standard CO_2 booster installation which performs similarly to the booster system with the parallel compression in colder climates such as in the UK (Gullo et al., 2017). Another key difference between the two models is the step-by-step approach adopted in the model of this paper for the increase of the condenser pressure in order to increase the amount of recoverable heat depending on the heat requirements of the buffer vessel. On the other hand, the model of D'Agaro, Coppola & Cortella (2019) switches directly to the maximum allowable pressure for additional heat recovery when heat supplementation to the buffer tank is required. Both studies, however, indicate that significant energy savings can be achieved by integrating thermal storage tanks into CO_2 booster refrigeration systems to provide exclusively the space heating to the supermarkets.

5. Conclusions

This paper investigated the potential of a CO_2 booster refrigeration integrated heating and cooling system with thermal storage for the provision of both space heating and cooling to the food cabinets of a UK supermarket. Its performance was compared to conventional heating and cooling solutions involving a gas boiler in terms of operating costs and GHG emissions. This was achieved by developing a theoretical one-dimensional implicit finite difference thermal storage model, which was then integrated into a CO_2 booster refrigeration model developed by Sarabia Escriva et al. (2019) in order to simulate five different heating and cooling strategies. Heating demand data were obtained from a real supermarket in the West Midlands region of the UK.

The results suggest that the adoption of a refrigeration integrated heating and cooling system with thermal storage can lead to a decrease in annual GHG emissions and energy consumption by 13% and 18% respectively compared to a conventional heat recovery plus gas boiler solution. It is worth highlighting that results from cases 3 to 5, which consider a thermal storage system, indicate space heating requirements in supermarkets can be solely fulfilled by heat recovery solutions. Making it clear to key stakeholders in the food retail industry that eliminating the use of natural gas for heat provision is an option worth considering. However, the conventional solution (Case 1) with heat supplementation from a gas boiler and no thermal storage was the most cost-effective among the five strategies simulated with 2.2% lower energy costs compared to the refrigeration integrated heating and cooling system with thermal storage. In addition to increasing the ratio of useful to recoverable heat by 11-12%, the integration of thermal storage into a refrigeration integrated heating and cooling system was shown to alleviate some of the underheating issues associated with the provision of heating directly from the desuperheater heat exchanger of the refrigeration system based on discussions with industry. The size of the buffer vessel and consequently the maximum amount of heat that can be stored is constrained by the installed high-pressure compressor capacity. Although a larger vessel would enable the storage of more energy, a larger compressor capacity would also be required to maintain it above the specified minimum temperature for space heating provision during peak heating demand periods. These findings are valuable as they are informing engineering experts in the food retail industry how they should be designing and operating heat recovery systems in existing buildings.

The availability of reliable, detailed data from an actual integrated heating and cooling supermarket refrigeration system with thermal storage would create additional opportunities for the development of more accurate models. Of particular interest in this context are dynamic system models that overcome some of the limitations of quasi-steady models such as the one which is considered in this work. It would also enable the calibration and validation of theoretical models, including the one developed in this study. Furthermore, it would provide the opportunity to develop hybrid models involving both a thermodynamic approach and a data-driven approach. Undertaking research in this field should inform built environment engineers and refrigeration system specialist about the preferred settings where a refrigeration integrated heating and cooling system is worth installing.

Future studies should examine the effect on the performance of refrigeration integrated heating and cooling systems with thermal storage if the temperature of the store was maintained at 19 °C both during the opening and the closing hours. Currently, the temperature of the store is reduced to 16 °C during these times. A higher temperature during the night could potentially reduce the spikes of heating demand when the store opens and allow more thermal storage during the night. Lastly, further work should be carried out in order to optimize both the design and the component sizing of refrigeration integrated heating and cooling systems with thermal storage. Future work should also consider different sizes of supermarket stores and the associated implications in terms of available space and capital costs.

Acknowledgements

This research was supported by funds provided via the Imperial-Sainsbury's Supermarkets Ltd. partnership. This work also was supported by the UK Engineering and Physical Sciences Research Council (EPSRC) [grant number EP/P004709/1]. Emilio J. Sarabia gratefully acknowledges financial support from Universitat Politècnica de València Fellowship. Data supporting this publication can be obtained on request from cep-lab@imperial.ac.uk.

References

Alfa Laval (2014) Plate heat exchangers: The theory behind heat transfer. [Online]. Available from: www.alfalaval.com/globalassets/documents/microsites/heating-and-cooling-hub/alfa_laval_heating_and_cooling_hub_the_theory_behind_heat_transfer.pdf [Accessed: 16 February 2020].

Angrisani, G., Canelli, M., Roselli, C. & Sasso, M. (2014) Calibration and validation of a thermal energy storage model: Influence on simulation results. Applied Thermal Engineering. [Online] 67 (1–2), 190–200. Available from: doi:10.1016/j.applthermaleng.2014.03.012.

BEIS (2019) Updated energy and emissions projections: 2018 | Annex M: Growth assumptions and prices. [Online]. 2019. GOV.UK. Available from: www.gov.uk/government/publications/updated-energy-and-emissions-projections-2018 [Accessed: 16 February 2020].

Buckley, R.C. (2012) Development of an energy storage tank model. MSc Thesis. [Online]. Chattanooga, University of Tennessee. Available from: https://scholar.utc.edu/cgi/viewcontent.cgi?article=1007&context=theses [Accessed: 16 February 2020].

Bui, T. (2010) Explicit and implicit methods in solving differential equations. Honors Scholar Theses. [Online] Available from: https://opencommons.uconn.edu/srhonors_theses/119 [Accessed: 16 February 2020].

Colombo, I., Maidment, G.G., Chaer, I. & Missenden, J.M. (2011) Carbon dioxide refrigeration with heat recovery for supermarkets. International Journal of Low Carbon Technologies. [Online] 9 (1), 38–44. Available from: doi:10.1093/ijlct/cts040.

D'Agaro, P., Coppola, M.A. & Cortella, G. (2019) Field tests, model validation and performance of a CO2 commercial refrigeration plant integrated with HVAC system. International Journal of Refrigeration. [Online] 100, 380–391. Available from: doi:10.1016/j.ijrefrig.2019.01.030.

Danfoss (2010) Transcritical CO_2 refrigeration with heat reclaim. [Online]. 2010. Danfoss: Engineering tomorrow. Available from: www.danfoss.com/en-gb/service-and-support/case-studies/dcs/transcritical-CO2-refrigeration-with-heat-reclaim [Accessed: 16 February 2020].

Danfoss (2008) Transcritical refrigeration systems with carbon dioxide (CO_2): How to design and operate a small-capacity (< 10 kW) transcritical CO_2 system. [Online]. Available from: http://files.danfoss.com/TechnicalInfo/Rapid/01/Article/TranscriticalArticle/PZ000F102_ARTICLE_Transcritical%20Refrigeration%20Systems%20with%20Carbon%20Dioxide%20(CO2).pdf [Accessed: 16 February 2020].

Dark Sky API (2019) Dark Sky API: Documentation. [Online]. 2019. Available from: https://darksky.net/dev/docs [Accessed: 16 February 2020].

Davis, M. (2011) Finite Difference Methods. [Online]. Available from: wwwf.imperial.ac.uk/~mdavis/FDM11/LECTURE_SLIDES2.PDF [Accessed: 16 February 2020].

Efstratiadi, M., Acha, S., Shah, N. & Markides, C.N. (2019) Analysis of a closed-loop water-cooled refrigeration system in the food retail industry: A UK case study. Energy. [Online] 174, 1133–1144. Available from: doi:10.1016/j.energy.2019.03.004.

Fankhauser, S., Averchenkova, A. & Finnegan, J. (2018) 10 years of the UK climate change act. [Online]. p.43. Available from: www.lse.ac.uk/GranthamInstitute/wp-content/uploads/2018/03/10-Years-of-the-UK-Climate-Change-Act_Fankhauser-et-al.pdf [Accessed: 16 February 2020].

Ge, Y.T. & Tassou, S.A. (2011) Performance evaluation and optimal design of supermarket refrigeration systems with supermarket model "SuperSim". Part II: Model applications. International Journal of Refrigeration. [Online] 34 (2), 540–549. Available from: doi:10.1016/j.ijrefrig.2010.11.004.

Gullo, P., Hafner, A. & Cortella, G. (2017) Multi-ejector R744 booster refrigerating plant and air conditioning system integration – A theoretical evaluation of energy benefits for supermarket applications. International Journal of Refrigeration. [Online] 75, 164–176. Available from: doi:10.1016/j.ijrefrig.2016.12.009.

Gullo, P., Tsamos, K., Hafner, A., Ge, Y. & Tassou, S.A. (2017) State-of-the-art technologies for transcritical R744 refrigeration systems – a theoretical assessment of energy advantages for European food retail industry. Energy Procedia. [Online] 123, 46–53. Available from: doi:10.1016/j.egypro.2017.07.283.

IPCC (2014) Summary for Policymakers. In: Climate Change 2014: Mitigation of Climate Change. Contribution of Working Group III to the Fifth Assessment Report of the Intergovernmental Panel on Climate Change. [Online]. Cambridge, UK and New York, Cambridge University Press. p. Available from: www.ipcc.ch/site/assets/uploads/2018/02/ipcc_wg3_ar5_summary-for-policymakers.pdf [Accessed: 16 February 2020].

Karampour, M. & Sawalha, S. (2016a) Integration of heating and air conditioning into a CO_2 transcritical booster system with parallel compression Part I: Evaluation of key operating parameters using field measurements. [Online]. Available from: doi:10.18462/iir.gl.2016.1049.

Karampour, M. & Sawalha, S. (2016b) Integration of heating and air conditioning into a CO_2 transcritical booster system with parallel compression Part II: Performance analysis based on field measurements. In: [Online]. 22 August 2016 p. Available from: doi:10.18462/iir.gl.2016.1052.

Karampour, M. & Sawalha, S. (2014) Performance and control strategies analysis of a CO_2 transcritical booster system. [Online]. Available from: https://www.researchgate.net/publication/281583942_Performance_and_control_strategies_analysis_of_a_CO2_trans-critical_booster_system [Accessed: 16 February 2020]

Lamb, R. (2018) Improving the energy efficiency of cooling systems. [Online]. 2018. Star Refrigeration. Available from: www.star-ref.co.uk/smart-thinking/improving-the-energy-efficiency-of-cooling-systems.aspx [Accessed: 16 February 2020].

Linde Gas (2019a) R32. [Online]. 2019. Available from: www.linde-gas.com/en/products_and_supply/refrigerants/hfc_refrigerants/r32/index.html [Accessed: 16 February 2020].

Linde Gas (2019b) R152a. [Online]. 2019. Available from: www.linde-gas.com/en/products_and_supply/refrigerants/hfc_refrigerants/r152a/index.html [Accessed: 16 February 2020].

MarketsandMarkets (2019) Transcritical CO_2 systems market by function, application and region - 2023 | MarketsandMarkets™. [Online]. 2019. Available from: www.marketsandmarkets.com/Market-Reports/transcritical-CO2-market-201387678.html# [Accessed: 16 February 2020].

Markides, C., White, M. & Handagama, N. (2017) Cooling with carbon dioxide. Energy World. 28–29.

Mateu-Royo, C., Karampour, M., Rogstam, J. & Sawalha, S. (2018) Integration of geothermal storage in CO2 refrigeration systems of supermarkets. In: [Online]. 2018 International Institute of Refrigeration. pp. 1265–1272. Available from: http://urn.kb.se/resolve?urn=urn:nbn:se:kth:diva-236385 [Accessed: 20 January 2020].

Mibec (2019) Bespoke buffer tanks by Mibec for large heating and cooling projects. [Online]. 2019. Mibec. Available from: https://mibec.co.uk/products/thermal-storage/bespoke-buffer-tanks [Accessed: 16 February 2020].

Mylona, Z., Kolokotroni, M., Tsamos, K.M. & Tassou, S.A. (2017) Comparative analysis on the energy use and environmental impact of different refrigeration systems for frozen food supermarket application. Energy Procedia. [Online] 123, 121–130. Available from: doi:10.1016/j.egypro.2017.07.234.

Nash, A.L., Badithela, A. & Jain, N. (2017) Dynamic modeling of a sensible thermal energy storage tank with an immersed coil heat exchanger under three operation modes. Applied Energy. [Online] 195, 877–889. Available from: doi:10.1016/j.apenergy.2017.03.092.

Nöding, M., Fidorra, N., Gräber, M. & Köhler, J. (2016) ECOS 2016: Operation Strategy for Heat Recovery of Transcritical CO2 Refrigeration Systems with Heat Storages. In: [Online]. Available from: https://pdfs.semanticscholar.org/db57/436f1cbb981ee7549607abf39fc6f312774d.pdf [Accessed: 16 February 2020]

Polzot, A., D'Agaro, P. & Cortella, G. (2017) Energy analysis of a transcritical CO_2 supermarket refrigeration system with heat recovery. Energy Procedia. [Online] 111, 648–657. Available from: doi:10.1016/j.egypro.2017.03.227.

Raccanello, J., Rech, S. & Lazzaretto, A. (2019) Simplified dynamic modeling of single-tank thermal energy storage systems. Energy. [Online] 182, 1154–1172. Available from: doi:10.1016/j.energy.2019.06.088.

Rahman, A., Fumo, N. & Smith, A.D. (2015) Simplified Modelling of Thermal Storage Tank for Distributed Energy Heat Recovery Applications. In: Volume 2: Photovoltaics; Renewable-Non-Renewable Hybrid Power System; Smart Grid, Micro-Grid Concepts; Energy Storage; Solar Chemistry; Solar Heating and Cooling; Sustainable Cities and Communities, Transportation; Symposium on Integrated/Sustainable Building Equipment and Systems; Thermofluid Analysis of Energy Systems Including Exergy and Thermoeconomics; Wind Energy Systems and Technologies. [Online]. 28 June 2015 San Diego, California, USA, ASME. p. V002T13A005. Available from: doi:10.1115/ES2015-49170.

Raka Adrianto, L., Grandjean, P.A. & Sawalha, S. (2018) Heat Recovery from CO2 Refrigeration System in Supermarkets to District Heating Network. In: [Online]. 2018 p. Available from: http://urn.kb.se/resolve?urn=urn:nbn:se:kth:diva-236090 [Accessed: 20 January 2020].

Sarabia Escriva, E.J., Acha, S., LeBrun, N., Francés, V.S., Pinazo Ojer, J.M., Markides, C.N. & Shah, N. (2019) Modelling of a real CO_2 booster installation and evaluation of control strategies for heat recovery applications in supermarkets. International Journal of Refrigeration. [Online] 107, 288–300. Available from: doi:10.1016/j.ijrefrig.2019.08.005.

Sawalha, S. (2008) Carbon dioxide in supermarket refrigeration. [Online]. Stockholm, Energiteknik, Energy Technology, Kungliga Tekniska högskolan. Available from: www.hysave.com/wp-content/uploads/2017/05/Carbon-Dioxide-in-Supermarket-Refrigeration.pdf [Accessed: 16 February 2020].

Sawalha, S. (2013) Investigation of heat recovery in CO_2 transcritical solution for supermarket refrigeration. International Journal of Refrigeration. [Online] 36 (1), 145–156. Available from: doi:10.1016/j.ijrefrig.2012.10.020.

Shi, L., Ferreira, C.A.I., Gerritsen, J. & Kalkman, H. (2017) Control strategies of CO_2 refrigeration / heat pump system for supermarkets. 10. Available from: http://hpc2017.org/wp-content/uploads/2017/05/O.1.1.4-Control-strategies-of-CO2-refrigeration-heat-pump-system-for-supermarkets.pdf [Accessed: 16 February 2020].

Skacanova, K.Z. & Gkizelis, A. (2018) Technical report on energy efficiency in HFC-free supermarket refrigeration. [Online]. Available from: https://issuu.com/shecco/docs/2018_kcep_shecco_eia_technical_repo [Accessed: 16 February 2020].

Tassou, S.A., Ge, Y., Hadawey, A. & Marriott, D. (2011) Energy consumption and conservation in food retailing. Applied Thermal Engineering. [Online] 31 (2), 147–156. Available from: doi:10.1016/j.applthermaleng.2010.08.023.

The Biomass Hut (2019) Buffer tanks. [Online]. 2019. Available from: www.thebiomasshut.co.uk/buffer-tank-distributor-uk-and-thermal-stores/renewable-energy--buffer-tanks [Accessed: 16 February 2020].

The Carbon Trust (2010) Refrigeration road map. [Online]. 2010. Available from: https://www.epa.gov/sites/production/files/documents/refrigerationroadmap.pdf [16 February 2020].

TRNSYS (2019) TRNSYS: Transient system simulation tool. [Online]. 2019. Available from: http://www.trnsys.com/index.html [Accessed: 16 February 2020].

UK Government (2019) Greenhouse gas reporting: Conversion factors 2019. [Online]. 2019. GOV.UK. Available from: www.gov.uk/government/publications/greenhouse-gas-reporting-conversion-factors-2019 [Accessed: 16 February 2020].

Wallace, K. (2013) Supermarkets for the future: Natural refrigeration and heat recovery. [Online]. p.51. Available from: www.cibse.org/getmedia/8366acbd-19d2-417c-b1b8-a1db9c6f8587/KEN-DALE-REPORT-KW-13-01-14.pdf.aspx [Accessed: 16 February 2020].